

FACTORS AFFECTING ANCHOR BOLT DEVELOPMENT

by

D. W. Lee and J. E. Breen

Research Report Number 88-1F

Research Project Number 3-5-65-88
Anchor Bolt Development

Conducted for

The Texas Highway Department

In Cooperation with the
U. S. Department of Commerce, Bureau of Public Roads

by

CENTER FOR HIGHWAY RESEARCH
THE UNIVERSITY OF TEXAS
AUSTIN, TEXAS

August 1966

ACKNOWLEDGMENTS

The tests described herein were conducted as a part of the overall research program at The University of Texas Center for Highway Research under the administrative direction of Dean John J. McKetta. The work was sponsored jointly by the Texas Highway Department and the Bureau of Public Roads under an agreement between The University of Texas and the Texas Highway Department. Liaison with the Texas Highway Department was maintained through the contact representative Mr. DeLeon Hawkins. Mr. I. C. Daniel was the contact representative for the Bureau of Public Roads. The study was directed by John E. Breen, Associate Professor of Civil Engineering, and supervised by Dong Woo Lee, Research Engineer, Center for Highway Research.

PREFACE

The results of the initial phase of a research program to study design criteria for the proper lengths for anchor bolt embedment into drilled shafts were reported by The University of Texas Center for Highway Research in April, 1964. Interpretation of the results of 36 anchor bolts with varying embedment conditions indicated that many important aspects of behavior were not sufficiently documented. In June, 1965, the research program was reactivated by The University of Texas Center for Highway Research in cooperation with the Texas Highway Department and Bureau of Public Roads. The program extension included a series of tests on 26 anchor bolts with varying embedment conditions. Major variables included the effect of the method of test, effect of clear cover, effect of low-cycle repeated loading, and effect of shape of the shaft. This report presents the results of these tests and a survey of the trends indicated thereby.

The opinions, findings, and conclusions expressed in this publication are those of the authors and not necessarily those of the Bureau of Public Roads.

FACTORS AFFECTING ANCHOR BOLT DEVELOPMENT

Introduction

The general purpose of this program was to investigate the influence of various factors affecting the development of the tensile yield capacity of high strength steel anchor bolts. Relatively little information is available concerning the design of large diameter anchor bolts which are extensively utilized in drilled shaft supports for highway sign structures. Limited information existing regarding concentric pull-out tests as recorded by Abrams (1)* and by Shoup and Singleton (2) is not particularly applicable to this case. The previous investigation by Breen (3) indicated that the results of concentric pull-out tests do not reflect the actual behavior of anchor bolt elements subjected to combined stress conditions and with limited clear cover. Working with ASTM A7 steel anchor bolts, Breen concluded that bolts with diameters of $1\frac{1}{4}$ " to 2" could be fully developed with a ten diameter embedment length, while a 15 diameter embedment length was required for 3" bolts. He also pointed out that the anchorage device was the most important element in developing the tensile strength of the anchor bolt and that only a minor portion of the bolt development could be credited to friction bond. Because of the limits on the range of variables studied, he recommended extension of the program in order to reach more conclusive design recommendations.

The present program was planned as a continuation of Breen's tests to investigate the following six fundamental variables:

1. Effect of method of loading
2. Effect of clear cover
3. Effect of low-cycle repeated loading
4. Effect of circular shape of drilled shafts
5. Effect of low concrete strength
6. Effect of 90-degree bends as anchorage devices

*Numbers in parentheses refer to corresponding numbers in the Bibliography.

In the previous project the test specimen shown in Fig. 1 was developed to simulate the behavior found in typical sign support structures. The bolt is embedded near the edge and tension is applied through flexural loading. In this type of specimen the concrete around the anchor bolt is under a combination of tension, bond, and splitting conditions somewhat approximating those in the prototype structure. However, the shear distribution is different because of the absence of a soil pressure distribution. This method of test was modified for the present investigation, as shown in Fig. 2, at the suggestion of the Bureau of Public Roads representatives, so that no lateral reaction was applied to the specimen in the length of the anchor bolt. This loading more realistically reflects the reaction conditions actually experienced in drilled shafts in service installations.

This investigation reports tests of 13 shaft specimens containing a total of 26 high strength bolts. The anchor bolt diameters were $1\frac{1}{4}$ " and 2" with embedment lengths of 10 diameters. End anchorages consisted of a standard nut except for one series in which the anchorage was a 90-degree bend.

Object and Scope

The object of this investigation was to evaluate the effect of various factors influencing the development of high strength anchor bolts in drilled shaft specimens.

The main factors investigated were:

1. Method of loading. The method of loading was modified at the suggestion of the Bureau of Public Roads to closely simulate field loading conditions.
2. Anchor bolt steel yield point. In place of the A7 steel used in the previous tests a high strength steel with a minimum specified yield strength of 60 ksi was used for all anchor bolts. The use of high strength bolts provided an opportunity to observe a greater range of anchorage characteristics and provided information for possible

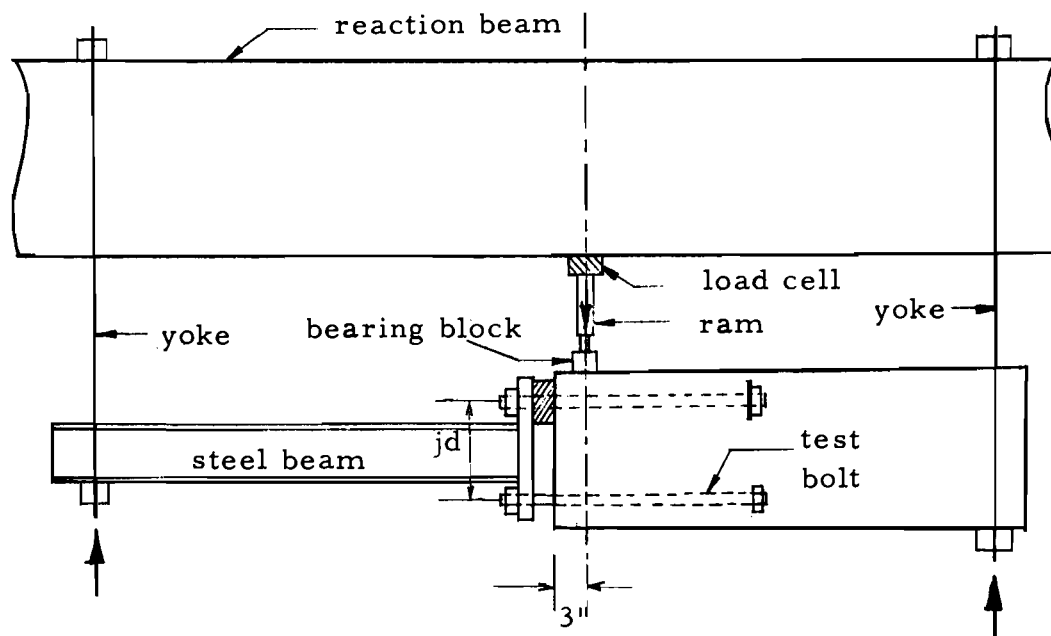


Fig. 1. Test arrangement for previous test program and series F of this program

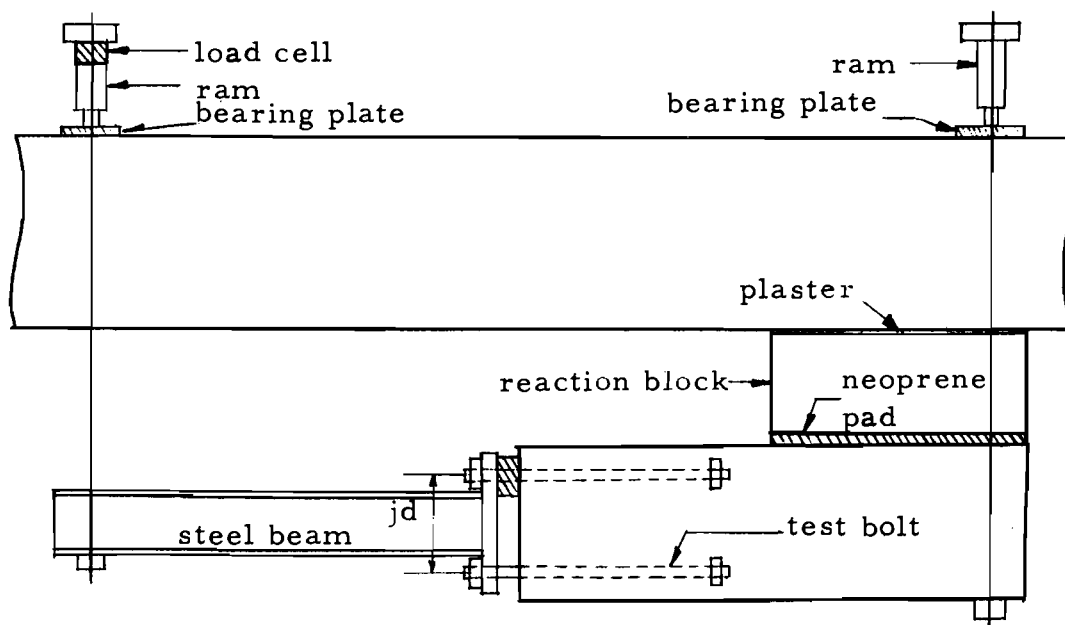


Fig. 2. Modified test arrangement for present series A-E

applications of high strength steel bolts under some design conditions.

3. The effect of clear cover. Four bolts of each size were tested with different clear cover to bolt diameter ratios. Ratios of 1.0, 1.9, 3.0, and 4.0 were used for $1\frac{1}{4}$ " diameter bolts. The 1.9 ratio was selected to provide a companion specimen to the previous tests to check any effect of the modification in the method of loading. Ratios of 1.0, 1.5, 2.5, and 3.5 were used for the 2" diameter bolts. The ratio 1.5 had been used in the previous series for this diameter.
4. Effect of low-cycle repeated loading. Two bolts of each size were tested to determine if cumulative slip at moderate overloads becomes an important design factor. Fifty cycles of static loading and unloading from 2 ksi to 34 ksi were imposed before final testing to failure.
5. Effect of circular shape. Two bolts of each diameter were tested in circular drilled shaft specimens, rather than square specimens. Since many bolts are embedded in circular footings and shafts, this is an important practical check.
6. Effect of low concrete strength. Two bolts of each size were tested in drilled shaft specimens with f'_c of about 2500 psi to check the effect of abnormally low compressive strength concrete.
7. Effect of 90-degree bends as anchorages. Since some designers prefer to anchor their bolts by providing 90-degree bends and bolt extensions rather than nuts or bolt heads, two bolts of each size were tested with this type anchorage.

Specimens

All of the shaft specimens used in this program were the same general type of square-sections used in the previous tests, except for the two circular-shape specimens. Two anchor bolts were cast in each shaft. The individual anchor bolts were designated by three or four-part code symbols, depending upon the variables involved. The first number represents the nominal bolt diameter. This is followed by the letter A to F to designate the main variables as follows:

- A: Clear cover
- B: Low-cycle repeated loading
- C: Circular shape
- D: Low concrete strength
- E: 90-degree bends
- F: Method of loading

One of these letters is followed by a number which is the ratio of clear cover to bolt diameter. The final letter--a or b--indicates the first or second bolt specimen respectively, with the same variable. For example, 2B1.5a designates a specimen with a 2" diameter bolt, a 1.5 ratio of clear cover to bolt diameter, and which is designed to investigate the effect of low-cycle repeated loading. The "a" indicates that it is the first of two bolts in the shaft specimen. Figures 3 to 5 show the entire set of test specimens with critical dimensions. A tabulation of the important variables and summary of the test results is provided in Appendix Table A.

Materials

Concrete. A concrete conforming to Texas Highway Department "Class A" concrete (4) was used in all standard concrete strength test specimens. All specimens were cast with a job-mixed concrete. High early strength cement (Type III) was used with a cement factor of 5.5 sacks per cubic yard and a slump range of 3 to 4 inches. Maximum aggregate size was 1 inch. The water-cement ratio was 7 gallons per sack. The low strength concrete for series D was obtained by cutting the cement factor to 4 sacks

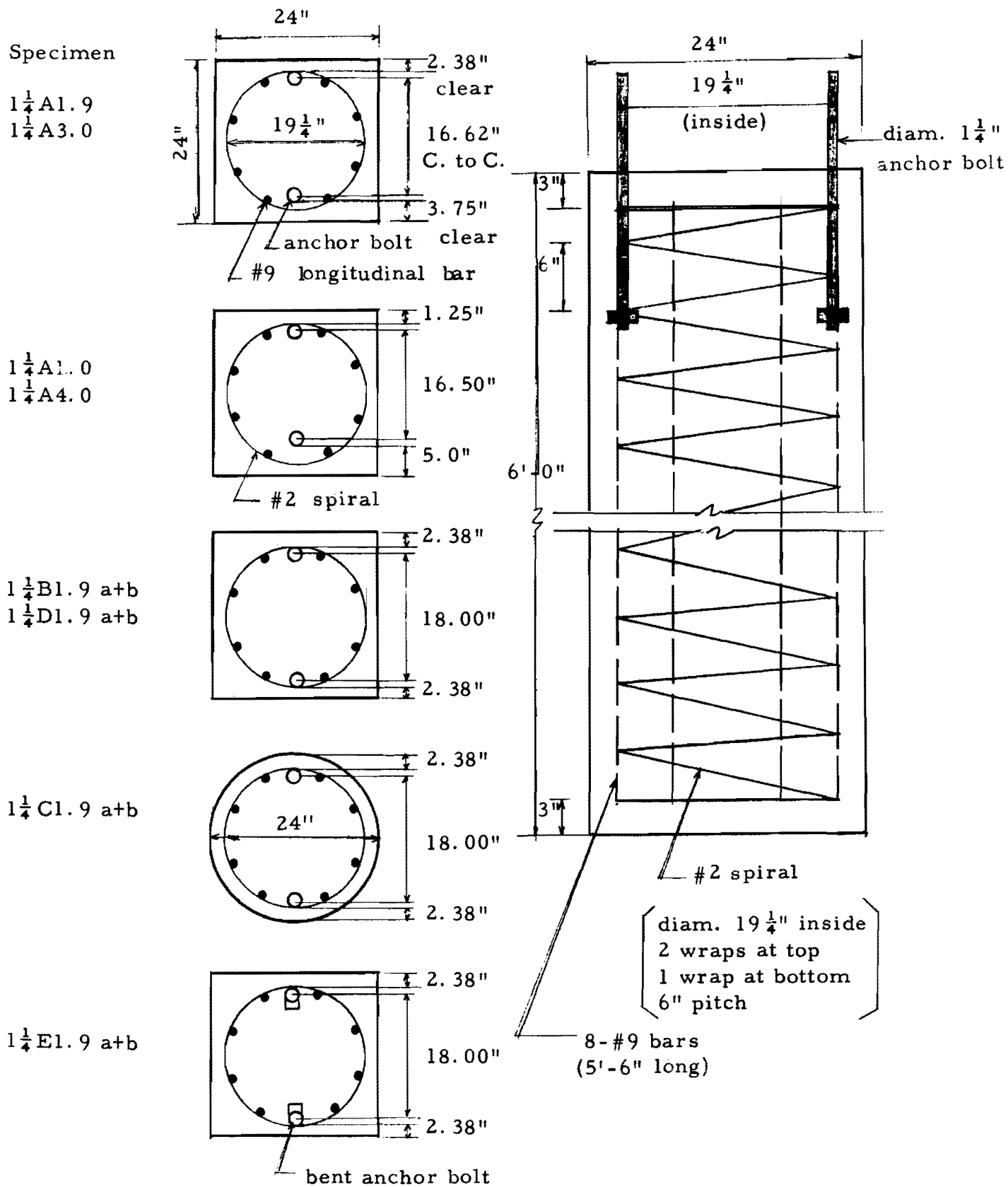


Fig. 3. Details of specimens with diameter 1 $\frac{1}{4}$ " bolts

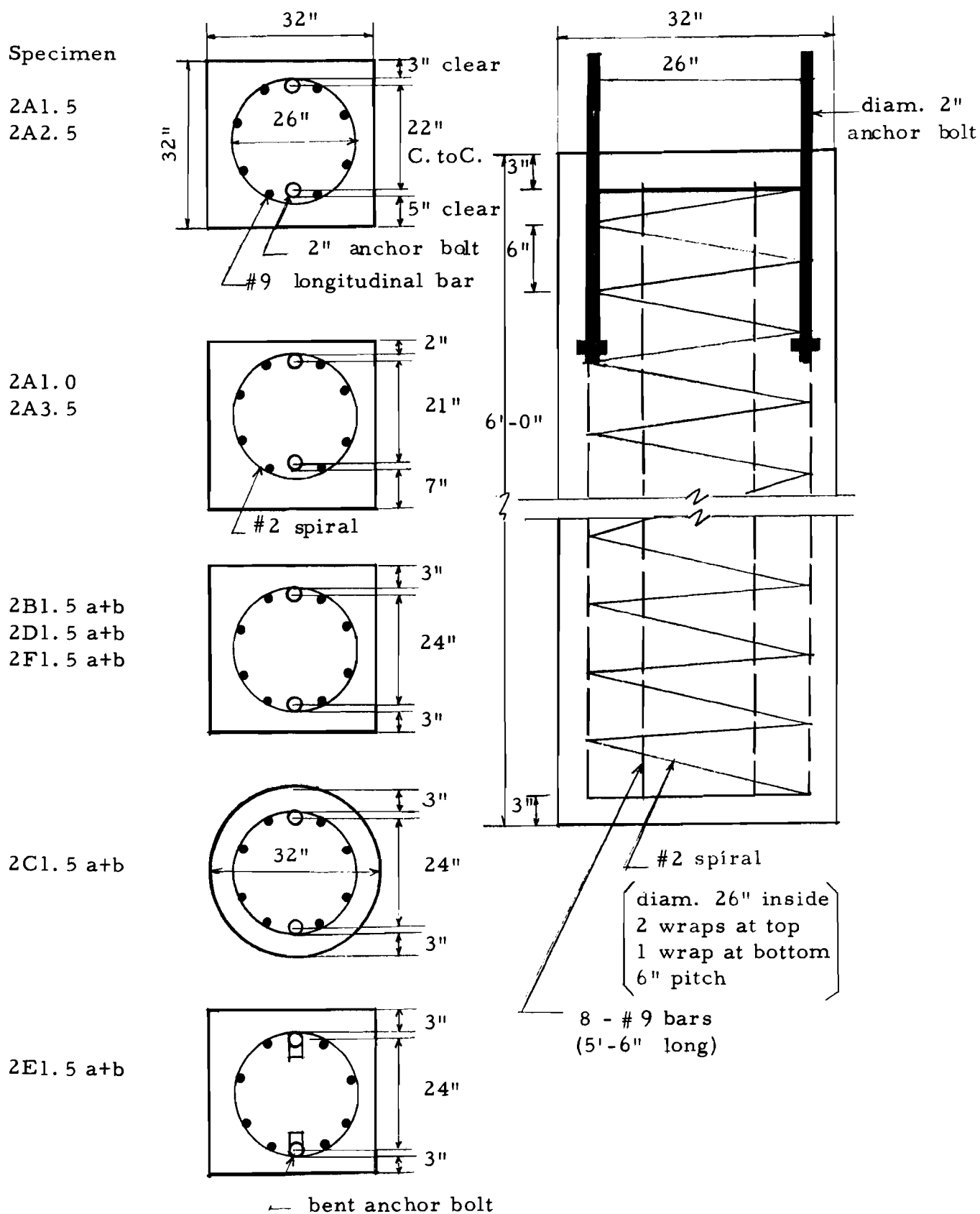


Fig. 4. Details of specimens with diameter 2" bolts

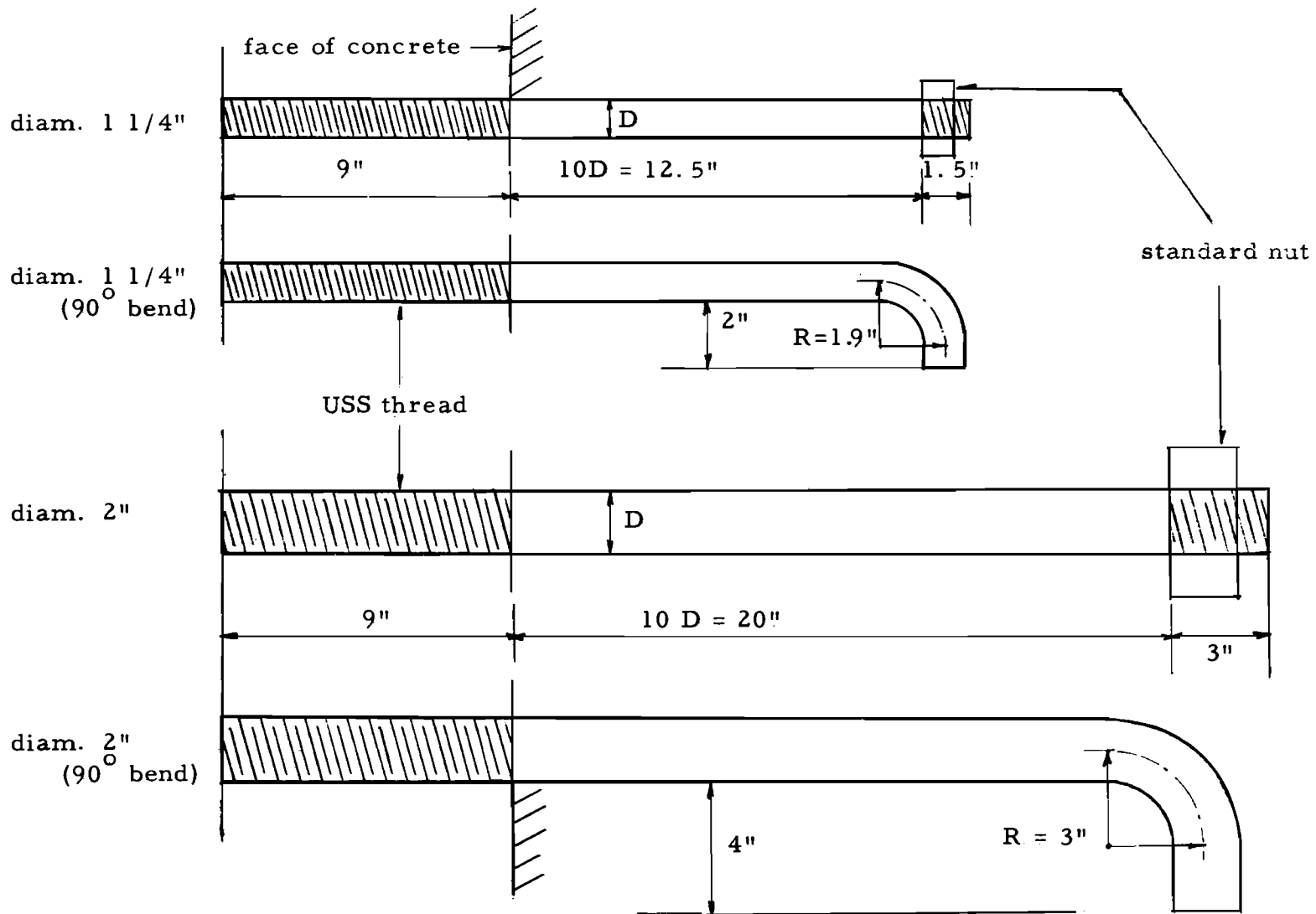


Fig. 5. Details of anchor bolts

per cubic yard and increasing the water-cement ratio to 10 gallons per sack with a 6 inch slump. The average compressive strength on the test date (at age seven days) was 4790 psi (excluding series D). The average compressive strength for cylinders for each specimen is given in Table A in the Appendix.

Anchor Bolts. The anchor bolts were specified to be manufactured from cold-rolled high strength steel, with a minimum yield strength of 60 ksi and a minimum elongation of 14 percent. The bolts were fabricated locally with USS threads from commercial grade 4142 cold-drawn, annealed, round bar stock and were not galvanized. The hooks for series E were bent after heating with a torch. Figure 6 shows the final shape of the bolts and Appendix Figure A shows typical stress-strain curves for the bolt stock used. The actual yield strengths at 0.002 offsets were 75 ksi for the 1½" diameter and 98 ksi for the 2" diameter bolts.

Reinforcing steel. The main reinforcing steel used met ASTM A305 and A15 intermediate grade specifications. The spirals were made from the same grade steel. The actual yield strengths from bars and spirals were 45 ksi and 46 ksi, respectively.

Forms. All specimens except those of circular shape were cast in wooden forms, as shown in Fig. 7. For the specimens of circular shapes special fiber forms were purchased from a local distributor. The bolts were fixed in a vertical position at the top of the forms and in all specimens the overall height was maintained at 6 feet to ensure that the water gain effect would remain relatively constant in all tests and would closely approximate that found under field conditions.

Neoprene pad. In order to provide a distributed reaction area between the specimen and the concrete reaction block, a 32" x 44" x ¾" Neoprene pad was utilized, as shown in Figs. 2 and 8.

Casting Procedure

The concrete was vibrated into place with a large internal vibrator. Standard compression test cylinders were cast from the batch which was placed



Fig. 6. Anchor bolts



Fig. 7. Form and cage

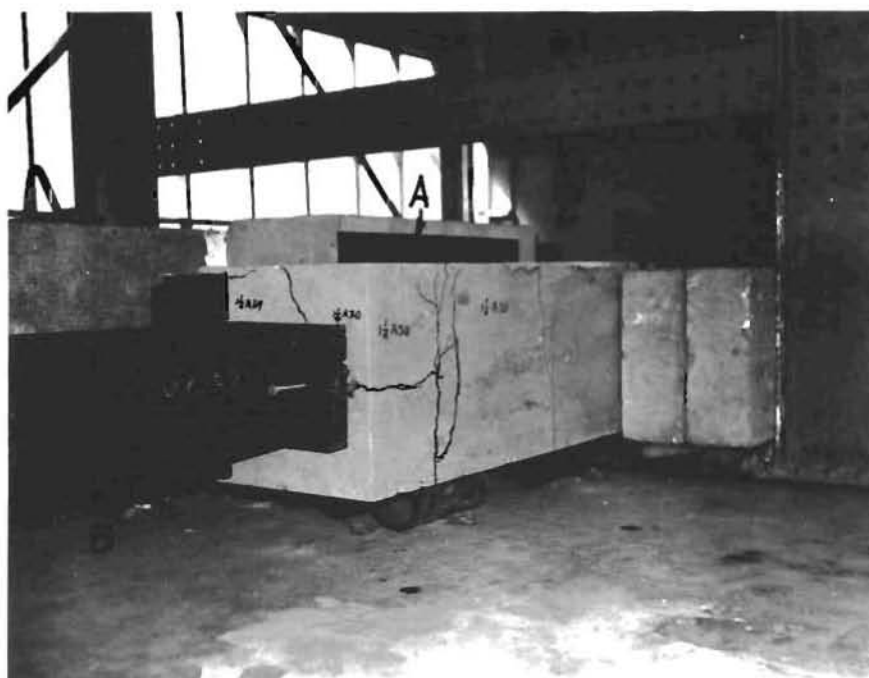


Fig. 8. Test arrangement with block and neoprene bearing pad

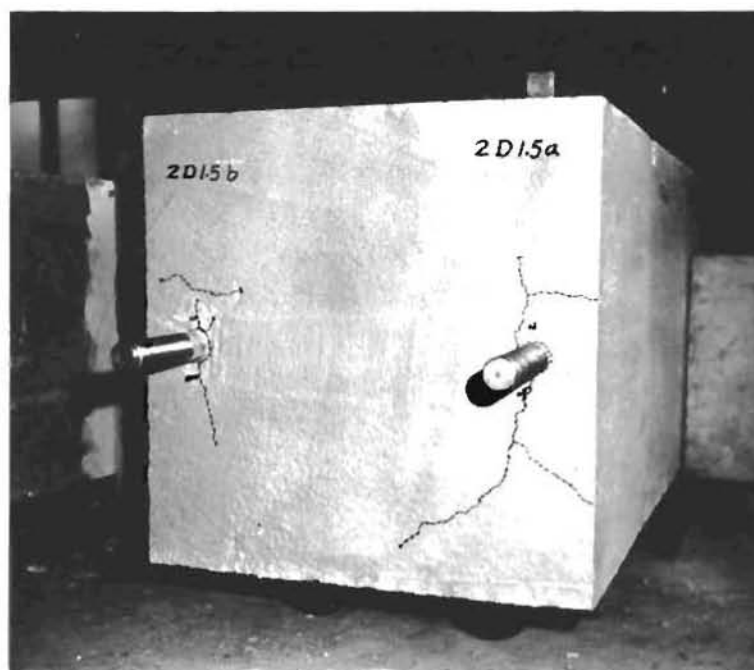


Fig. 9. Shrinkage cracking prior to testing

in the top portion of the specimen surrounding the test bolts. Because of the reasonable slumps used, good compaction was obtained.

Curing

The specimens were troweled and then left overnight in the form with a piece of plastic placed over the open end of the form. The next day the form was stripped for reuse and the specimen was left in the laboratory under burlap until the test date. Substantial shrinkage cracks were observed in one of the series D specimens (low concrete strength) as shown in Fig. 9. Some evidences of batch boundaries were found in most specimens after removing the forms.

Test Procedure

The general procedure used in loading involved some modification from the previous tests so that no lateral reaction would be applied to the specimen in the length of the anchor bolts, as shown in Fig. 2. The distributed reaction below the anchorage length was provided by a Neoprene pad inserted between the specimen and concrete reaction block, as shown in Figs. 8 and 10.

On the day of test, the specimen was moved to the testing position and mounted on large rollers. Before attaching a specially fabricated steel wide-flange section the drilled shaft specimen was fitted against the Neoprene pad as snugly as possible. After putting the wide-flange section on the specimen, the reaction straps were positioned to yoke the test assembly to the heavy reaction beam. A calibrated hydraulic ram and an electronic load cell were inserted between the reaction beam and reaction strap to supply a cantilever load (P-1) at the end of the wide-flange section, as shown in Fig. 11. Another calibrated ram was installed at the far end of the specimen to supply the reaction P-2, as shown in Fig. 12. The loads, P-1 and P-2, were applied proportionately except for a few initial loading increments when a low load P-2 was applied first in order to seat the specimen at the far end and secure a relatively rigid loading system. The

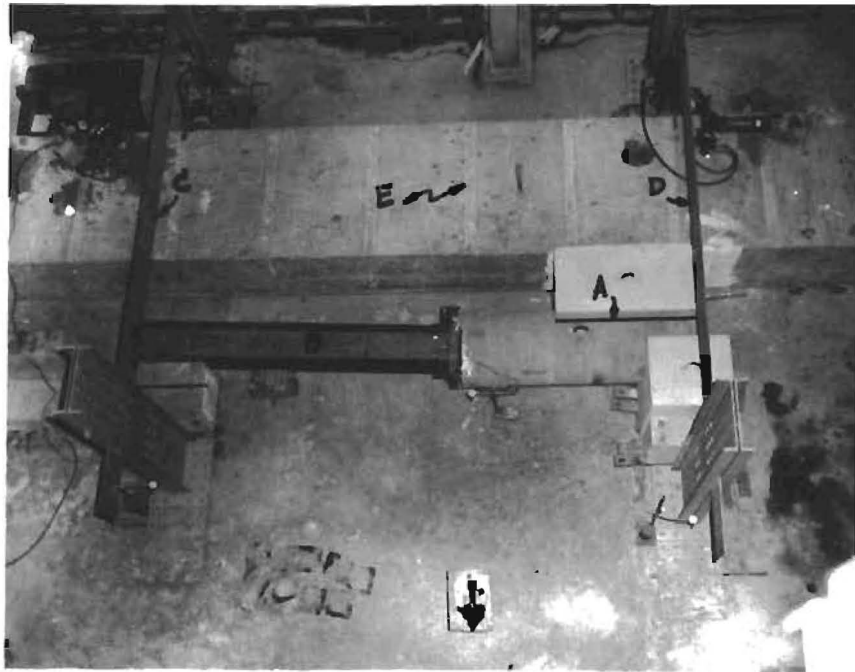


Fig. 10. General view of test arrangement

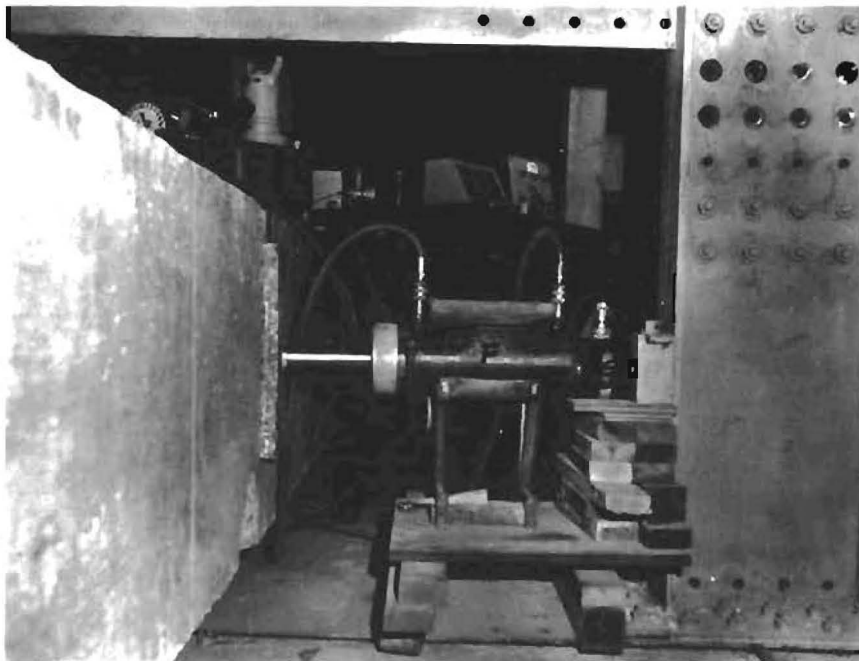


Fig. 11. Loading System

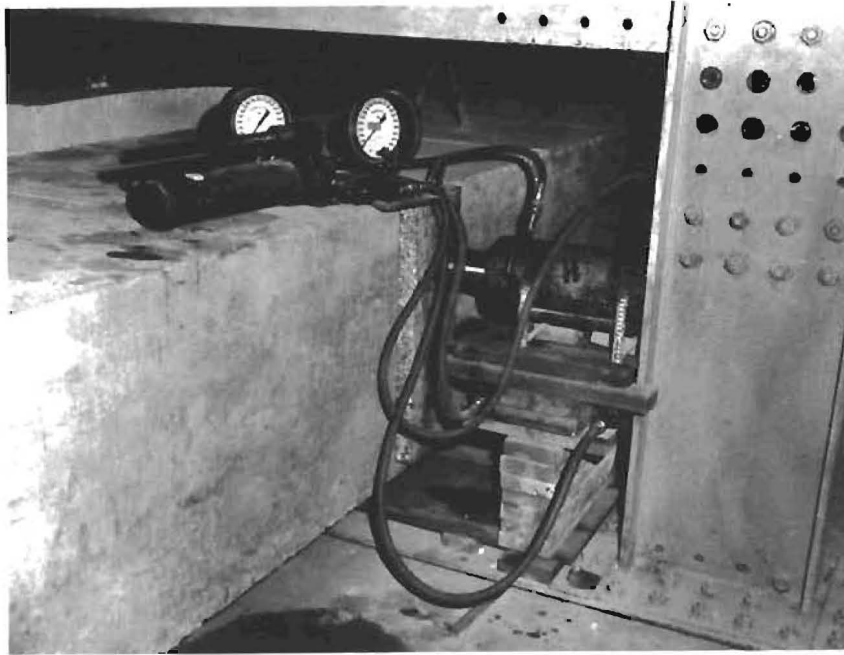


Fig. 12. P2 load equipment

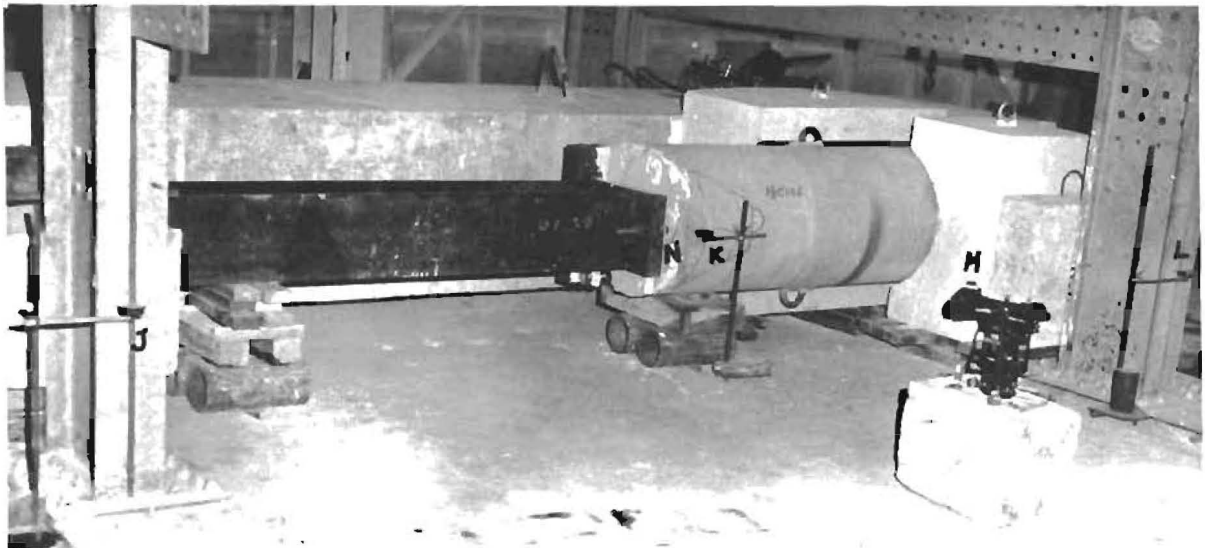


Fig. 13. Slip and deflection measurement equipment

values of the load P-2 were chosen so that the specimen was always subjected to distributed load across the entire Neoprene pad.

The instrumentation utilized was relatively simple. Dial gauges were used to measure the deflection of the reaction straps and near the head of the bolt an optical micrometer (mounted on the theodolite shown in Fig. 13) was used to measure the relative slip between the anchor bolt and the concrete face. Targets were mounted above and below the bolt on steel rods embedded in the concrete. A third target was mounted on the bolt 1/2" from the face of the concrete. The optical micrometer was used to read the relative displacement between the targets and had a sensitivity of 0.001 inches.

The loads were applied in increments and held until the instrumentation was read and any cracking recorded. Loading for a particular test required approximately one to two hours, except for the specimens of B series (repeated loading). Since each specimen contained only two anchor bolts, all bolts were tested to failure. For several specimens the concrete surrounding the initial bolt tested was so badly damaged that loading for the next bolt required the use of a thick steel plate for compression bearing. This reduced the moment lever arm and induced a small uncertainty in the exact magnitude of the arm.

Due to specific variables involved, further modifications were needed for the B and C series. For the B series (repeated loading) standard loading increments were used for the first cycle loading to an anchor bolt steel stress of 34 ksi. The bolts were then unloaded to 2 ksi by four decrements. From the second cycle to the fiftieth cycle, loading and unloading was done by two load increments and two load decrements between 2 ksi and 34 ksi. After the fiftieth cycle the standard load increments were resumed to failure. In the first test of this series all readings were taken for every load increment and decrement. It was found that the cumulative slip was very small. Since the testing time required was substantial, in all other tests readings were taken every fifth cycle.

For the C series (circular shaft specimens) the Neoprene pad was glued to a circular concave concrete reaction block, shown in Fig. 13, so that effective contact between the Neoprene pad and a reasonable surface of the specimen could be maintained.

Definitions and Basic Calculations

To avoid ambiguity in terminology used, certain definitions are required:

1. Slip - The total relative displacement of the target on the anchor bolt with respect to the face of the concrete. It includes true slip and some extension occurring in the original unbonded length of the bolt.
2. Mean stress area (A_{sm}) - To take into account the partially threaded anchor bolt, the mean stress area formula recommended by ASTM Standards (5) was used to calculate all steel stresses. For the present test series two mean stress area values were used (0.969 sq. in. for 1½" diameter bolt and 2.498 sq. in. for the 2" diameter bolt).
3. Mean steel stress (f_{sm}) - Steel stresses vary along the length of the anchor bolt in the shaft specimen. Considering the indeterminate state of stresses along the bolt due to the bond conditions, the mean steel stress is defined as the steel stress at the face of the concrete based on the mean stress area of the anchor bolt. Thus all steel stress can be calculated from the following formula:

$$f_{sm} = M/A_{sm} \text{ } jd$$

where M = bending moment at the face of the concrete
 A_{sm} = mean steel area
 jd = lever arm (see Fig. 2)

As the compressive force was concentrated on a very small line area of the compression zone the lever arm $j d$ was known within an accuracy of 5 percent; thus all mean steel stresses could be reasonably accurately calculated.

Specimen Behavior and Failure

Through the entire process of loading the general behavior was very similar for all specimens. Loaded end slip started almost immediately upon initial loading and progressed with gradually increasing increments. In all specimens definite flexural cracks appeared first across the side face of the specimen at the maximum bending moment section, which was 10 or 20 inches below the bolt anchorage and also was near the mix boundary of two of the batches. Approaching the ultimate load cracks developed parallel (splitting) and normal (flexural or crushing) to the axis of the drilled shaft specimen in the vicinity of the bolt anchorage. In most cases the normal cracks were observed before the parallel cracks became visible. Observation of the first parallel crack almost certainly indicated that the load was very close to ultimate.

Most of the specimens failed in the splitting failure mode, which Breen observed in his previous series (3). Several specimens showed slightly different patterns which will be discussed further in later sections. The three predominant failure patterns were classified as follows:

1. Splitting - Wide splitting cracks appeared along the full length of the bolt at ultimate and the concrete cover over the bolt was broken off into two distinct wedges, as shown in Fig. 14.
2. Edge splitting - In circular shape specimens the splitting cracks did not develop directly over the bolt axis. Instead, a single edge block was broken off by edge splitting, as shown in Fig. 15.
3. Crushing - Pronounced radial crushing cracks developed in the region around the bolt anchorage, as shown in Fig. 16.

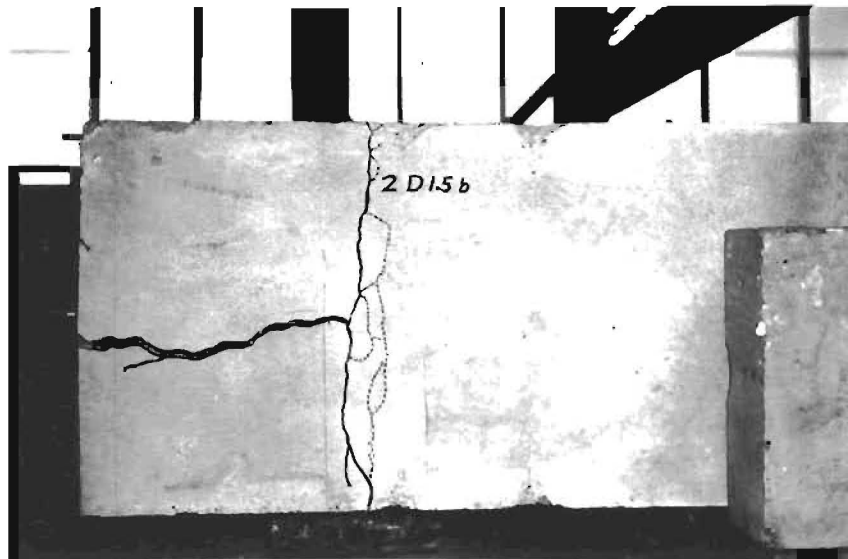


Fig. 14a. Splitting failure

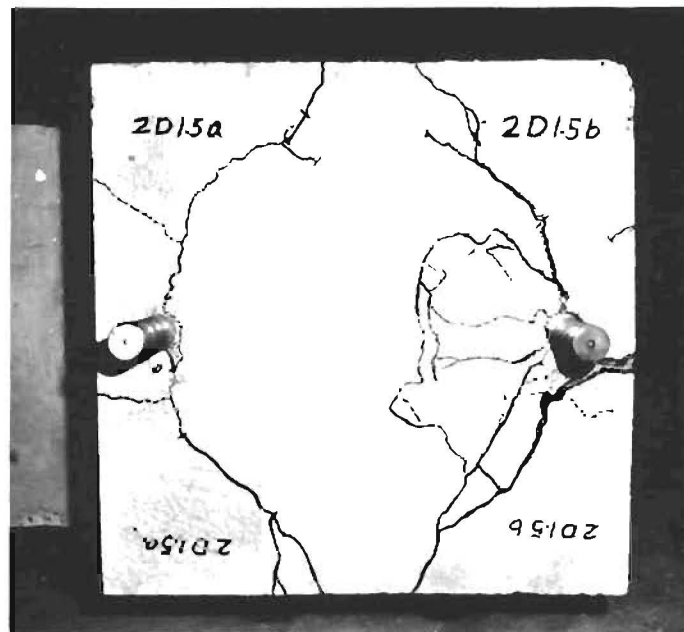


Fig. 14b. Splitting failure - end view



Fig. 15a. Edge splitting failure

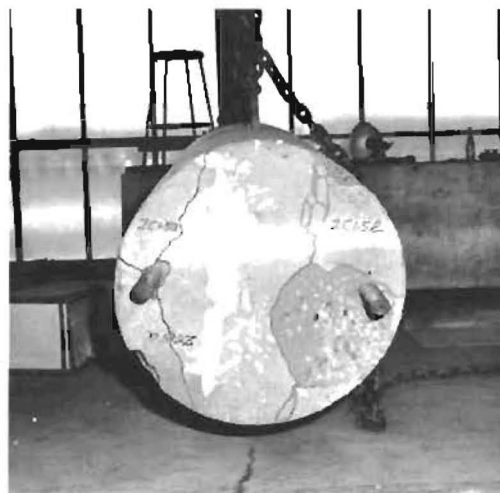


Fig. 15b. Edge splitting failure - end view

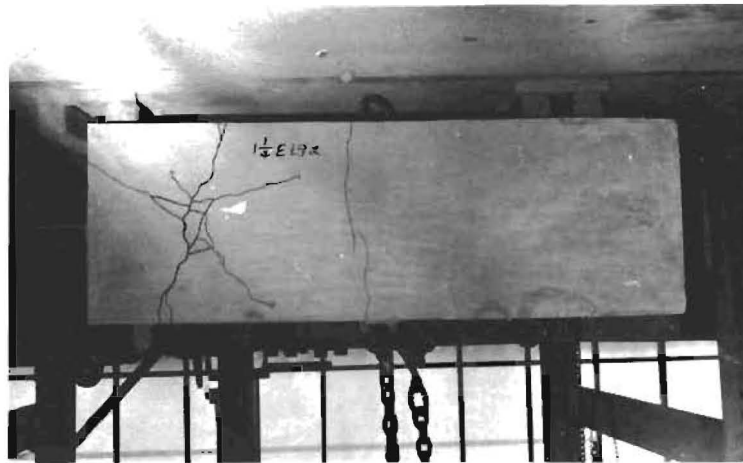


Fig. 16a. Crushing failure

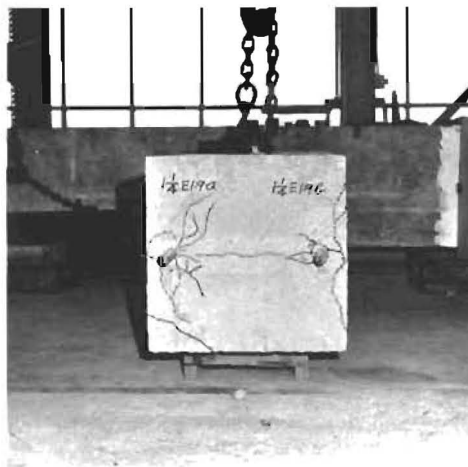


Fig. 16b. Crushing failure - end view

Minor splitting cracks developed, but did not extend along the full bolt length and distinct wedges did not form.

In contrast to the previous series utilizing ASTM A7 anchor bolts, the full ultimate tensile strength of the high strength anchor bolts of the present series was not developed in any specimen. In addition the nominal yield points (60 ksi) of the bolts were developed in only 35 percent of all the specimens tested.

Effect of Method of Loading

In order to more closely simulate the field loading conditions the method of test in the present program was modified from that of the previous program as shown in Figs. 1 and 2. Since the significance of the method of loading was unknown and was assumed to be relatively minor at the initial stage of the program, the change in the loading method was not planned as one of the major variables. However, a preliminary analysis of test data indicated a significant discrepancy in loaded end slip measurements between the two series although the developed ultimate bolt stresses were approximately the same magnitude. Because of the large discrepancy in slip values an additional series of specimens was added to specifically study the variance in the method of loading. The F series consisted of two 2" diameter high strength anchor bolts embedded in a single specimen. They provided exact duplicates of specimen 2A1.5, except that they were loaded with an edge reaction in the length of the anchor bolt (as shown in Fig. 1).

The magnitude of the discrepancy of slip measurements can be seen from the steel stress versus loaded end slip curves plotted in Fig. 17. The steel stress-slip curves for specimens 2N10a and b of the previous program agree very well with the comparable specimens of the F series of the present program. The higher steel stresses reached by the specimens of the F series are due to the higher strength steel used in the bolts. This agreement verified the accuracy of the test procedure and instrumentation calibrations utilized in the present program. In marked contrast, the steel stress-slip curve for the comparable specimen of the present program

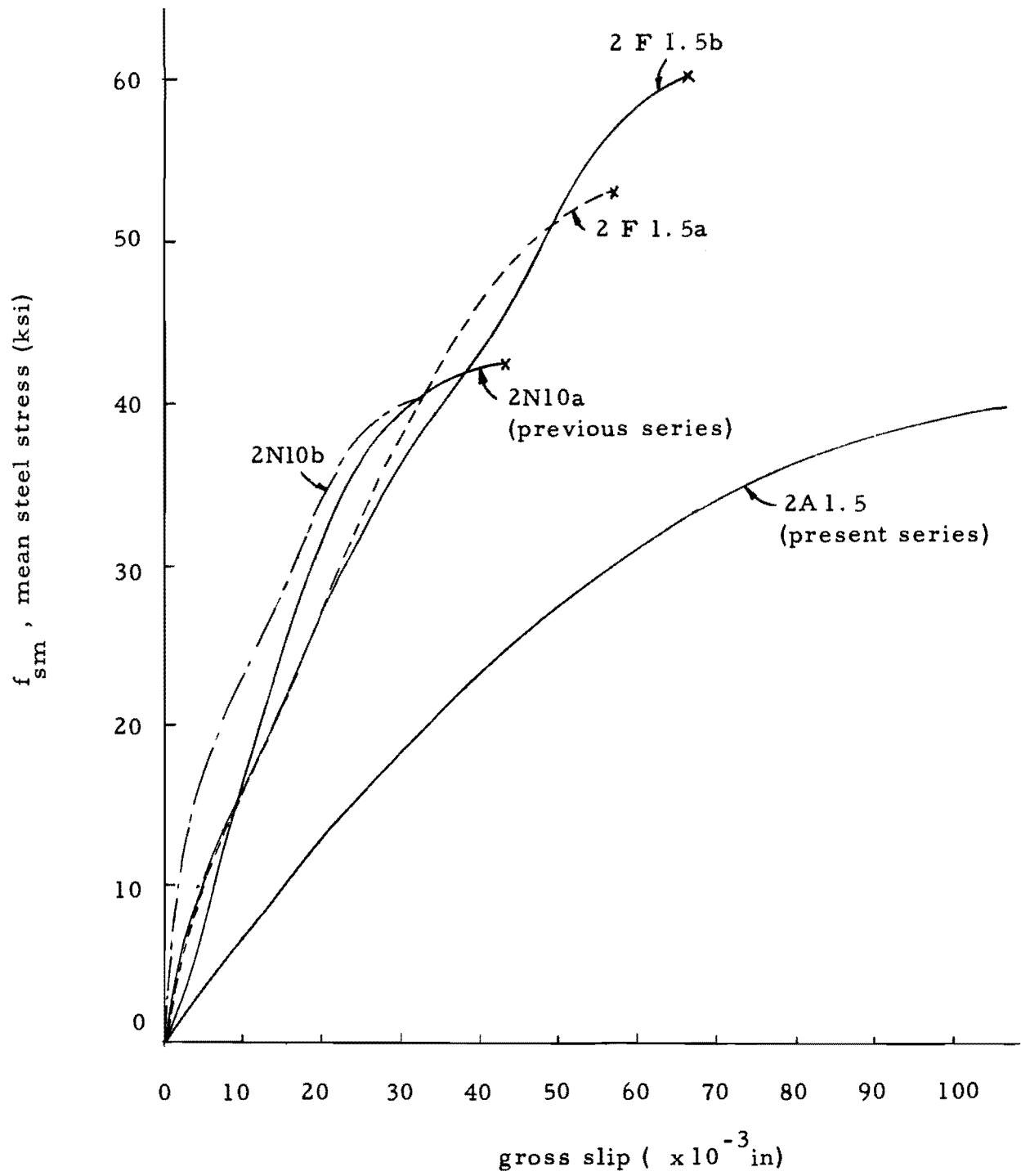


Fig. 17. Steel stress vs slip curves for different methods of test

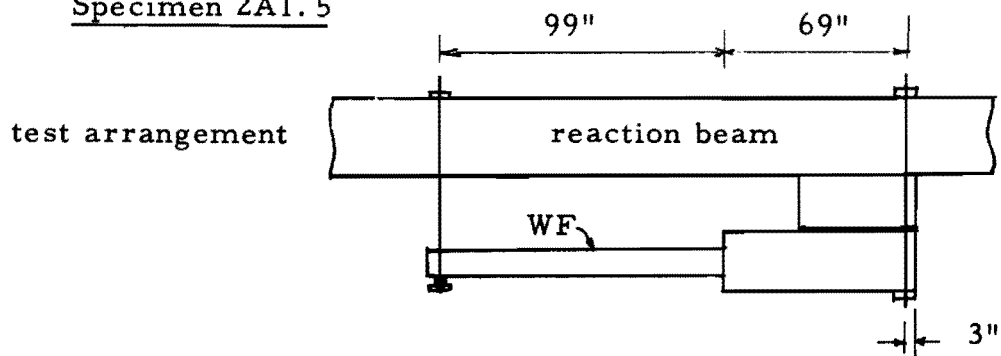
(2A1.5) indicates a slip magnitude about three times larger at any level of steel stress. The only difference between specimens 2A1.5 and 2F1.5 was the modification in the method of loading. This indicates that the method of loading significantly influences the slip behavior.

The gross slip measured in this program has three components:

1. The actual relative displacement between the anchor bolt and concrete which is normally considered the true slip.
2. The extension of that portion of the anchor bolt which was not originally embedded in concrete but which was included in the gauge length.
3. The effect of local concrete strains due to stress concentrations.

Because of the highly indeterminate character of the combined stress conditions along the anchor bolt, an exact quantitative check of slip is impossible. However, some approximate qualitative analysis can be made. Figures 18 and 19 show the shear, bending moment, and steel stress diagrams along with sketches of the method of loading for specimens 2A1.5a and 2F1.5a, respectively. The level of load shown corresponds to a mean steel stress at the loaded end of the anchor bolt of 20 ksi. The load distribution in the cantilever portion of the specimen is known from statics. However, the actual distribution of the bearing stress in the Neoprene pad is indeterminate and for the purpose of these computations has been assumed to be uniform. The exact nature of the distribution is of secondary importance in this discussion.

Several important aspects of these diagrams should be noted. In the former loading arrangement, as shown in Fig. 19, the maximum bending moment section is very close to the face of the shaft specimen. Most of the embedded length of the anchor bolt is in a region of gradually decreasing moment. In contrast the loading used in the present program (shown in Fig. 18) places the anchor bolt in a region of gradually increasing moment and the maximum moment section for the anchor bolt is at the anchorage end.

Specimen 2A1.5

For $f_{sm} = 20$ ksi

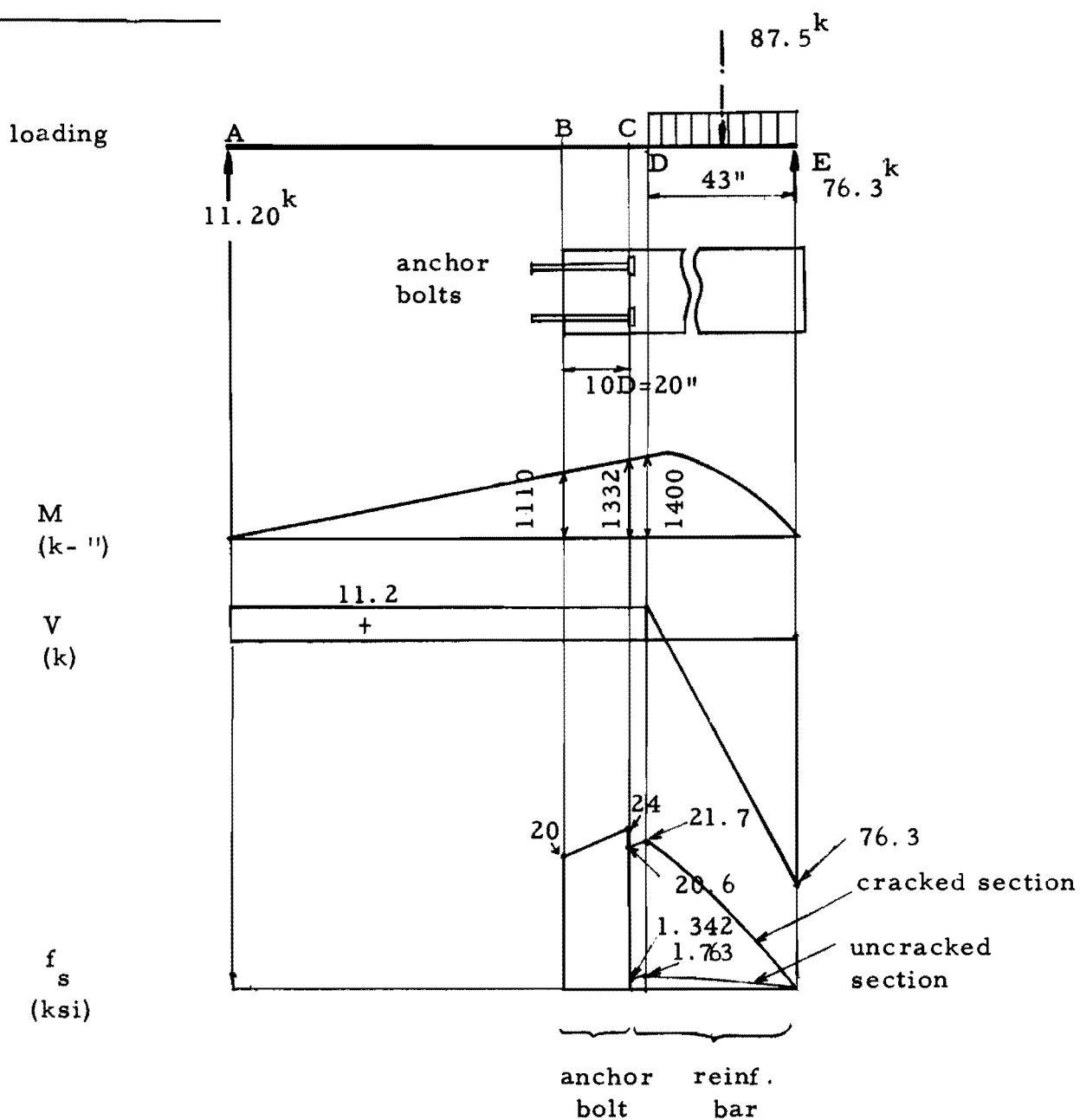


Fig. 18. Shear, bending moment, and steel stress diagrams for 2A1.5

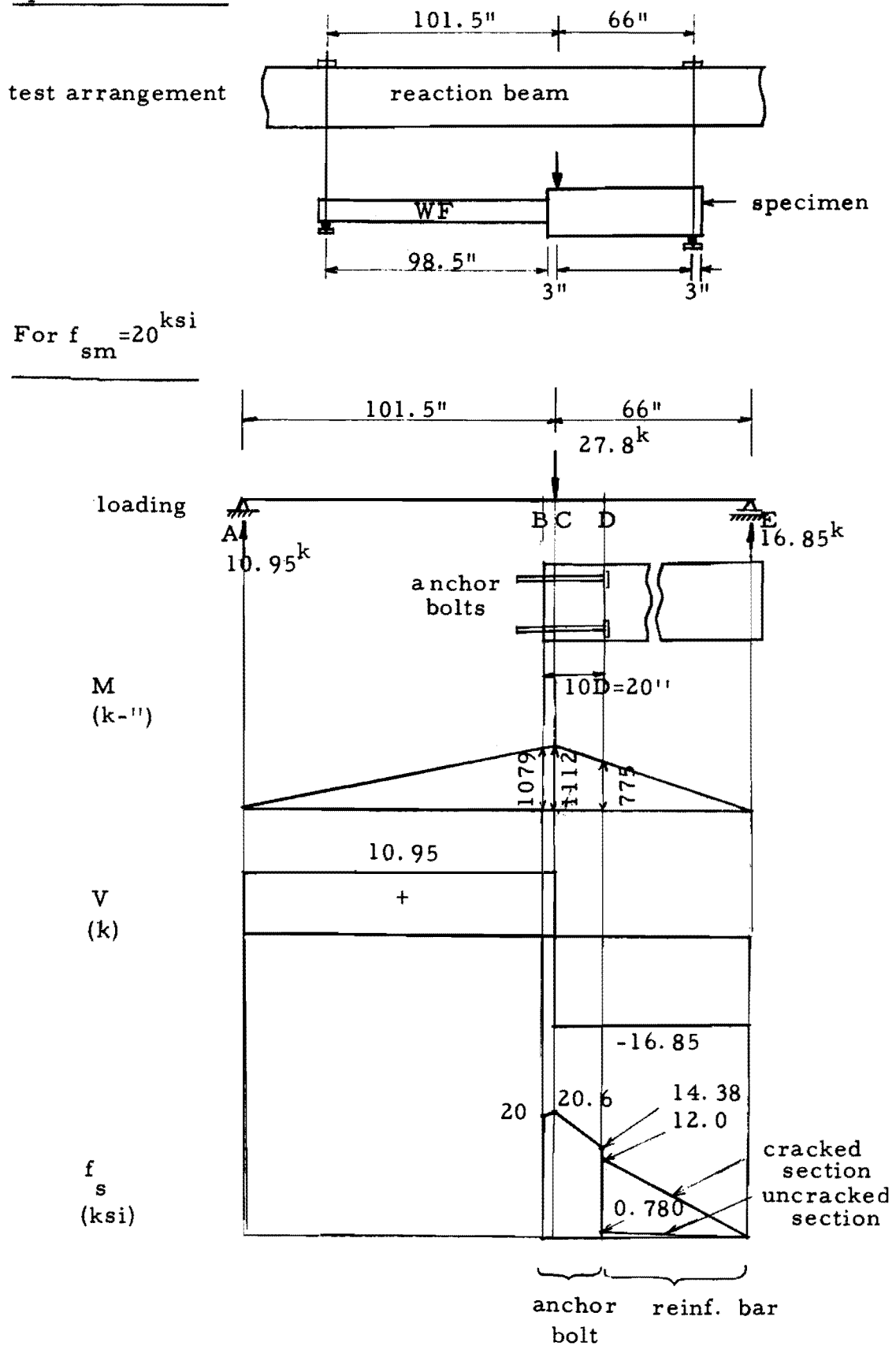
Specimen 2F1.5a

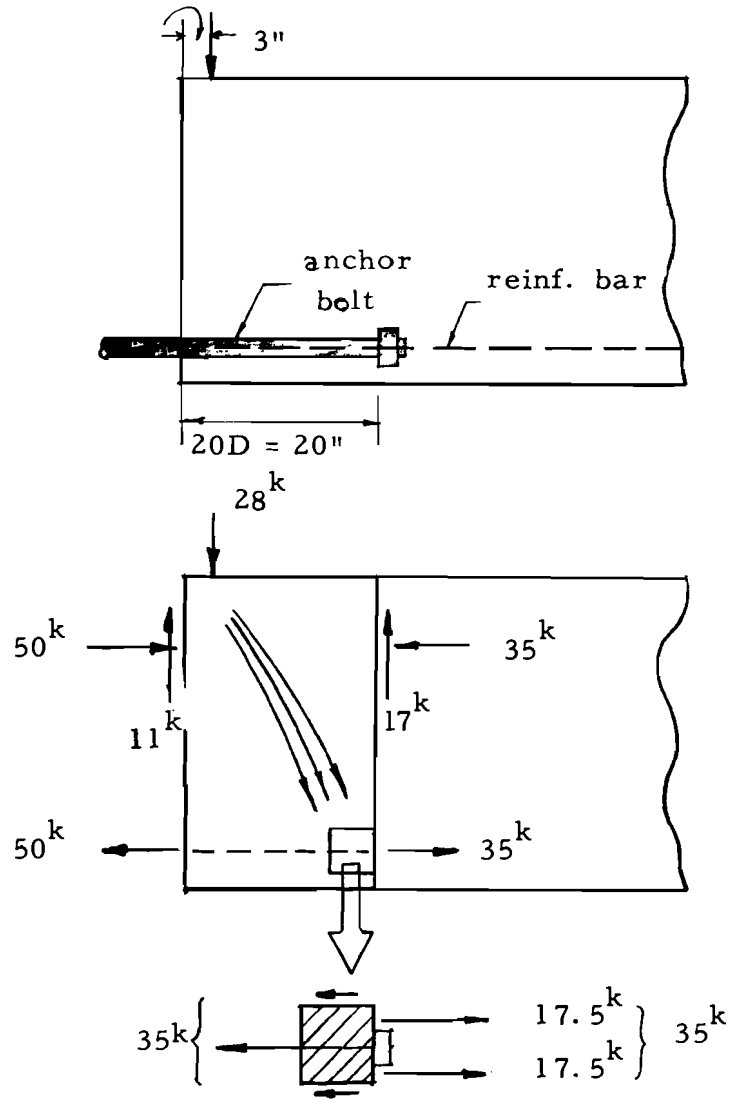
Fig. 19. Shear, bending moment, and steel stress diagrams for 2F1.5a

Comparison of the shear diagrams indicate that the full length of the bolt in specimen 2A1.5 is subjected to positive shear, whereas the greater part of the bolt length in specimen 2F1.5a is subjected to negative shear. These two conditions cause a great difference in the steel stress distribution in the anchor bolts. The exact distribution of steel stress along the bolt length cannot be known because of the complex bond stress transfer to the conventional reinforcement. However, since the major part of the transfer is involved around the anchorage, the stress calculations ignore reinforcement in the embedment length. From the steel stress diagrams, larger bolt extensions would be expected for the specimens of the present program at the same nominal end steel stress. While this factor offers some justification for the larger slips measured, the threefold magnitude of the discrepancy still seems too large.

For the same nominal steel stress level of 20 ksi free body diagrams for the two specimens are given in Fig. 20 to illustrate local stress and strain concentrations. Isolating small concrete elements in the vicinity of the bolt anchorages, the force acting on the element of 2A1.5 is almost twice as large as for 2F1.5a. This localized condition should cause a substantial difference in the magnitude of the local concrete strain in the anchorage region. In addition, the concentrated reaction applied in the embedded length in the previous program exerts a confining effect and tends to reduce the local concrete strain. There is no such confining factor in the embedded length of the anchor bolt in the present program. The absence of the confining effect of the concentrated reaction was observed during testing of the specimens in this program, since several specimens suffered shearing type failures in the compression bearing face and supplemental steel bearing plates had to be used to distribute the reactions. This complication had not been encountered to any substantial degree in the previous program. The absence of the confining pressure probably contributes to significantly increased slippage of the anchorage device itself and could account for a substantial portion of the difference in observed slip.

2F1.5a

$jd = 21 \frac{1}{4}"$
clear cover = 3"



2A1.5

$jd = 22 \frac{1}{4}"$
clear cover = 3"

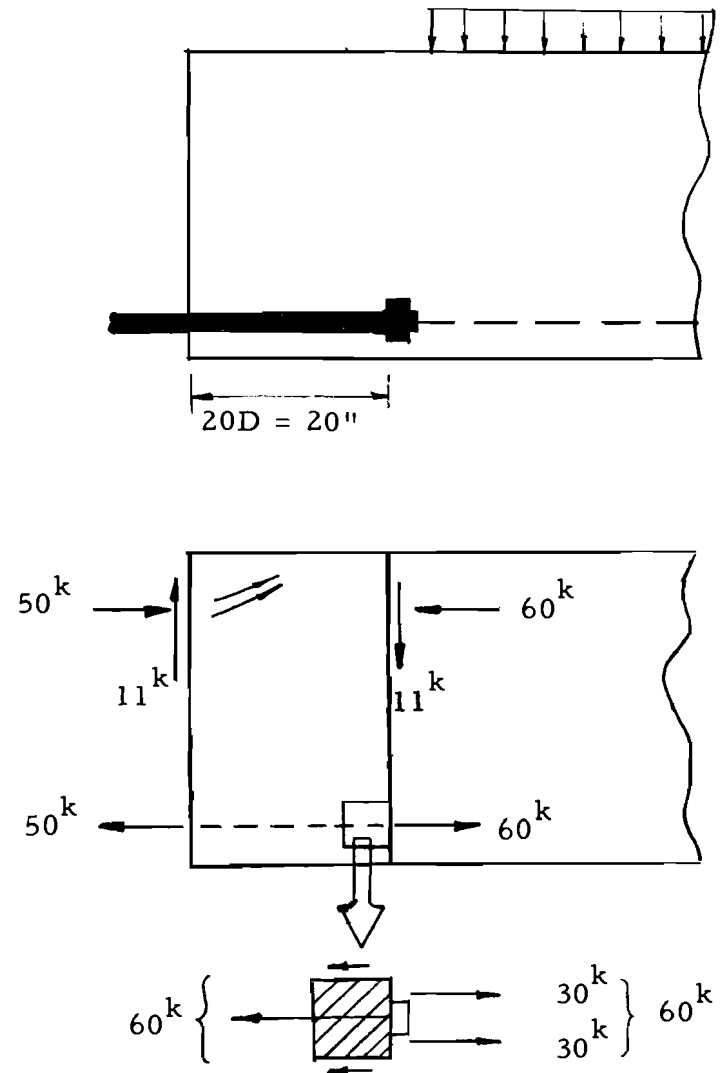


Fig. 20. Free-body diagrams

Comparisons of the magnitudes of slip for the different loading methods are also shown in Fig. 21, where gross slip versus bolt diameter diagrams are given for three steel stress levels. The individual points shown are the results of specimens in the present series, which include variations in cover, and other factors. The average value for the specimens in the previous program are shown by the dashed lines, while a solid line shows the computed elastic elongation of completely unbonded bolts. This plot indicates the significance of the method of loading on the measured slip. Since virtually all points from the present program fall above the line corresponding to the unbonded elastic elongation, it seems certain that movement in the anchorage vicinity associated with the local concrete strain contributes the major part of the total gross slip.

Similar test results were reported by Shoup and Singleton (2) while studying the anchorage behavior of stud anchors embedded in a massive beam and tested in axial tension. Their test was essentially a direct pull-out test, but they applied the tension force to the bolt in such a way that the concrete surface was free from external forces. Displacements were measured to show the amount of movement between the top surface of the concrete and the stud. The load versus displacement curves show that for steel stresses of approximately 20 ksi the measured displacement was twice as large as the unbonded elastic elongation of the anchor stud. These results tend to confirm the larger slips to be expected in the absence of confining pressures.

Effective Clear Cover

Analysis of the results of the previous investigation of this series indicated that the amount of concrete cover over the anchorage is a major parameter in the development of the ultimate strength of an anchor bolt. It was shown that the effective clear cover can be studied more readily by introducing the nondimensional parameter of clear cover to bolt diameter (C'/D). Since the range of this parameter had been limited from 0.83 to 1.9 in the previous investigation, it was decided to vary this ratio from 1.0 to 4.0 in the present series.

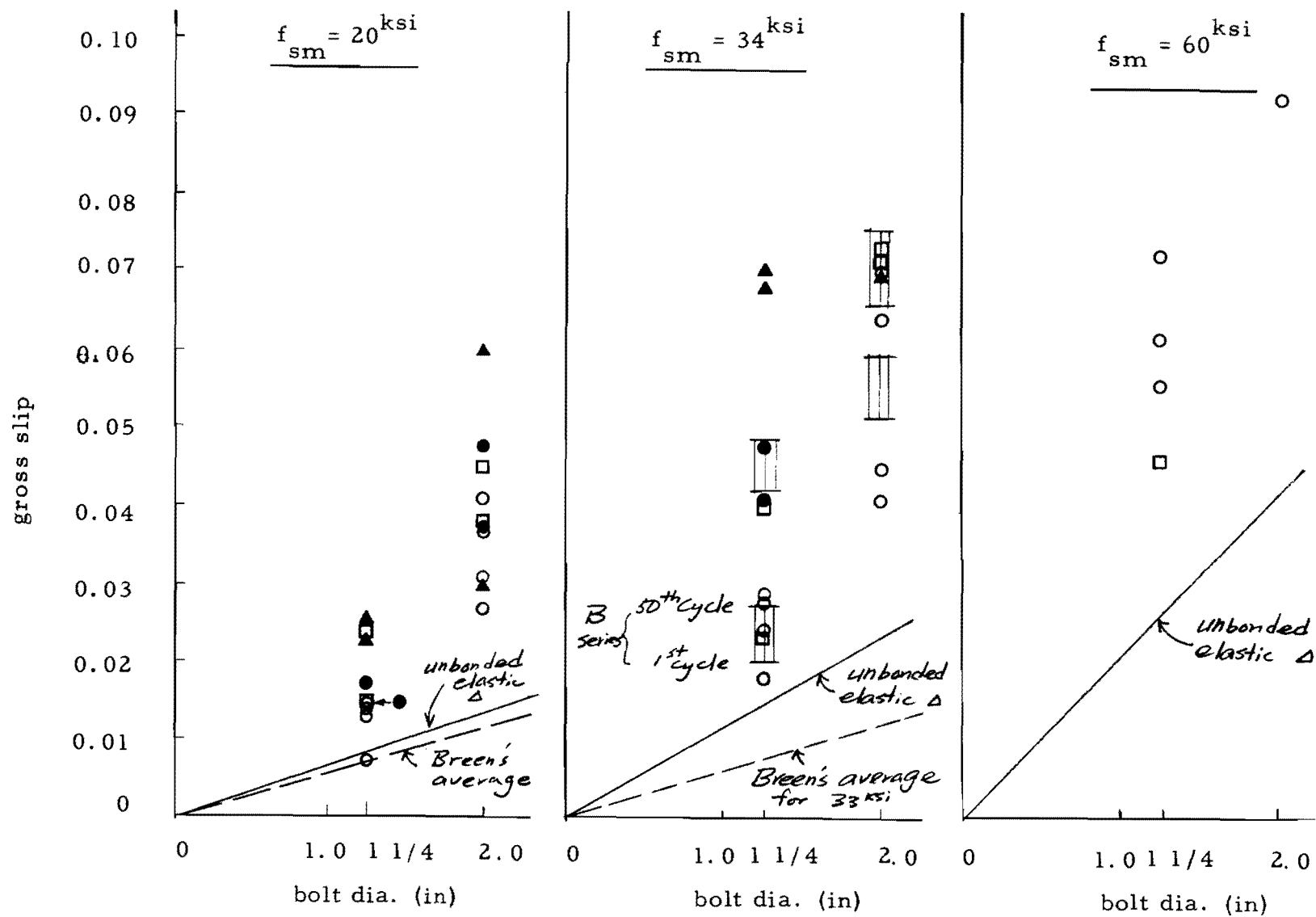


Fig. 21. Slip vs bolt diameter for steel stresses 20^{ksi}, 34^{ksi}, and 60^{ksi}

Figure 22 indicates the variation of failure patterns with increasing covers. For low ratios of clear cover to bolt diameter the failure patterns were primarily crushing with a lesser amount of splitting. Intermediate ranges indicate substantially larger amounts of splitting and relatively small amounts of crushing. In contrast, the higher ratios resulted in typical splitting failures with no evidence of crushing.

The effect of clear cover on the ultimate strength of the anchor bolts of the A series is shown in Fig. 23. There is a definite trend of increasing ultimate strengths with increased cover and some evidence of slightly higher strengths for the smaller size bolts. A similar plot for all bolts of the present program is shown in Fig. 24. The same general trends are indicated. Further discussion of this figure will be made in later sections of the report regarding the influence of individual parameters on the ultimate strength.

Since all failures in the present series were basically governed by concrete behavior, it is necessary to study relationships between concrete stresses and the cover provided. In a previous program Breen (3) postulated a hypothesis based on a semi-rational analysis and observation of the physical tests. He assumed that the critical stress area will occur not at the end anchor, but at the base of the cone defined where an imaginary cone of stresses intersects the surface of the specimen. This area was called the critical stress area and was computed as

$$A_{cr} = \frac{\pi}{4} (C^2 - D^2)$$

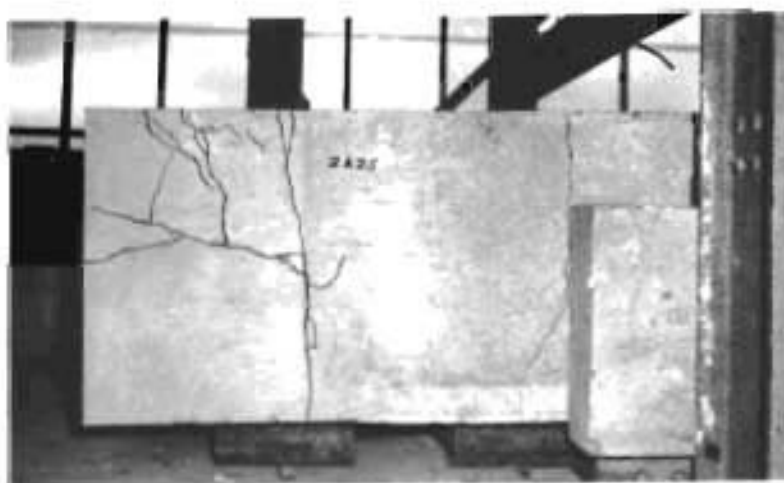
where $\frac{C}{2}$ = total cover measured from the center line of the bolt to the edge of the concrete, and

D = diameter of the bolt.

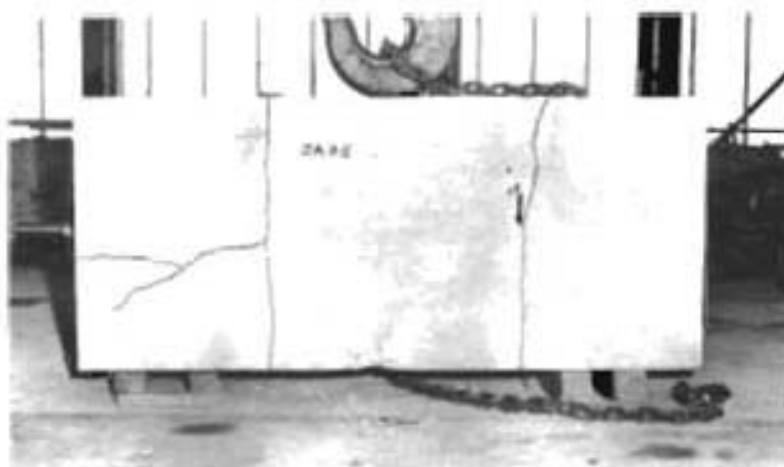
By computing the bearing stresses on this fictitious stress area, a new index was introduced which can be expressed as



crushing
 $C'/D=1.0$



crushing and
splitting
 $C'/D = 2.5$



splitting
 $C'/D=3.5$

Fig. 22. Failure patterns as influenced by varying covers

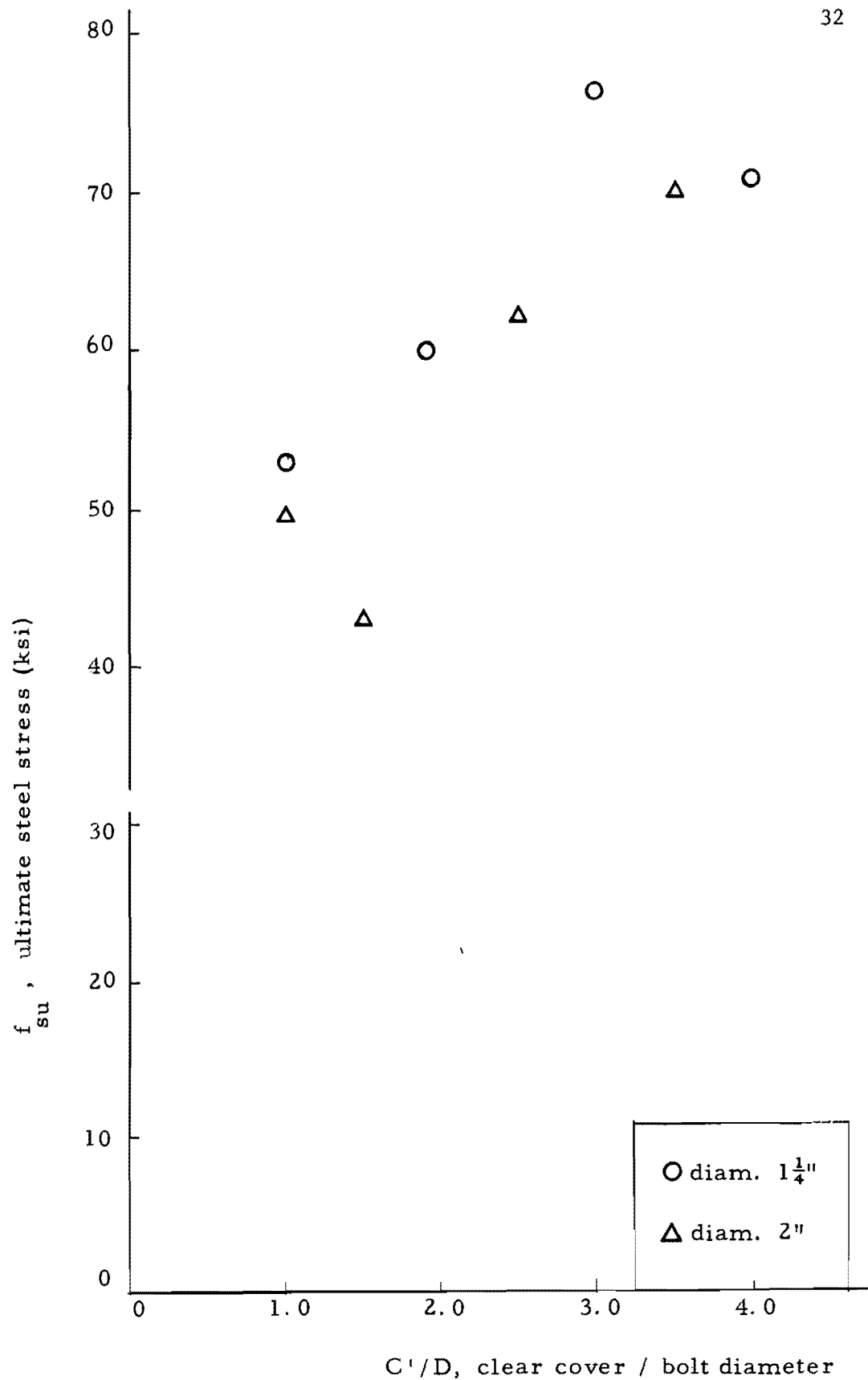


Fig. 23. Ultimate steel stress vs ratio of clear cover to bolt diameter (A series)

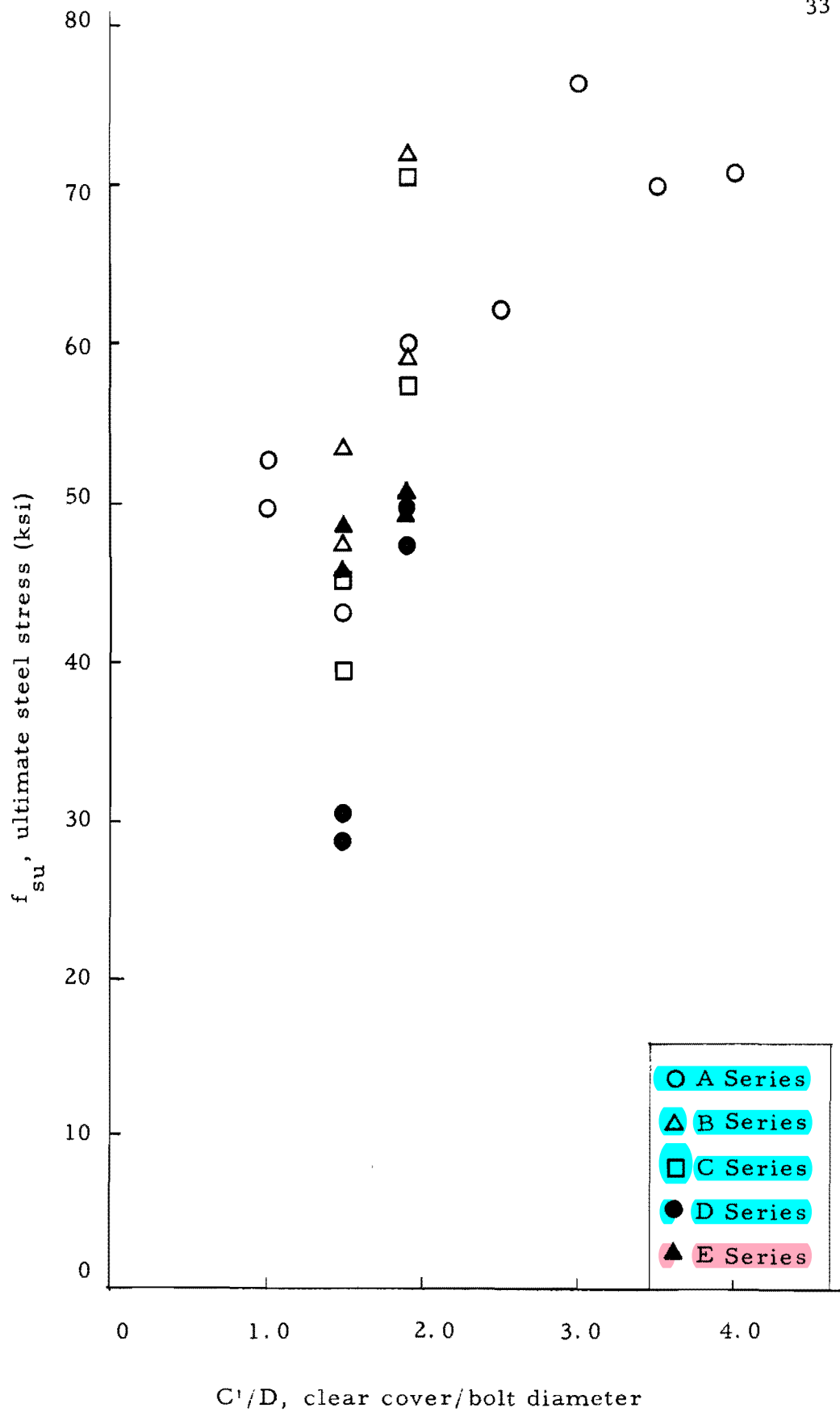


Fig. 24. Ultimate steel stress vs ratio of clear cover to bolt diameter (all series)

$$f_{su} A_{sm} = f_{cr} A_{cr}$$

or

$$f_{cr} = (A_{sm}/A_{cr})(f_{su})$$

The fictitious ultimate bearing stresses, f_{cr} , have been computed and are given in Appendix Table A. In order to recognize the variation of the concrete strength in the specimens, these stresses have been further corrected by dividing by $\sqrt{f'_c}$. All values of $f_{cr}/\sqrt{f'_c}$ are given in Appendix Table A.

Based on these results, Figs. 25, 26, and 27 are plotted. Figure 25 indicates the results of the A series, where the only variable was the amount of clear cover. Figure 26 includes the results of all series of the present program except the E series (90-degree bends). Figure 27 includes the results from the previous program as well as the present program. The data shown in these figures clearly confirm the hyperbolic curve trend predicted in the earlier study and extend its validity for a wide range of C'/D . Because of the scatter inherent in the data, it is possible to fit several different trend lines (as shown in Fig. 26). In order to obtain a conservative design expression relating the required concrete cover to develop a certain steel stress, the most conservative of the three expressions shown would be

$$(f_{cr}/\sqrt{f'_c})^{1.232} (C'/D) = 56.5$$

This equation was used with three different concrete strengths and six different bolt diameters to illustrate ultimate steel stress-clear cover relationships. The results are shown in Fig. 28. From these or similar curves the required clear cover to develop a desired steel stress can be determined for various concrete strengths.

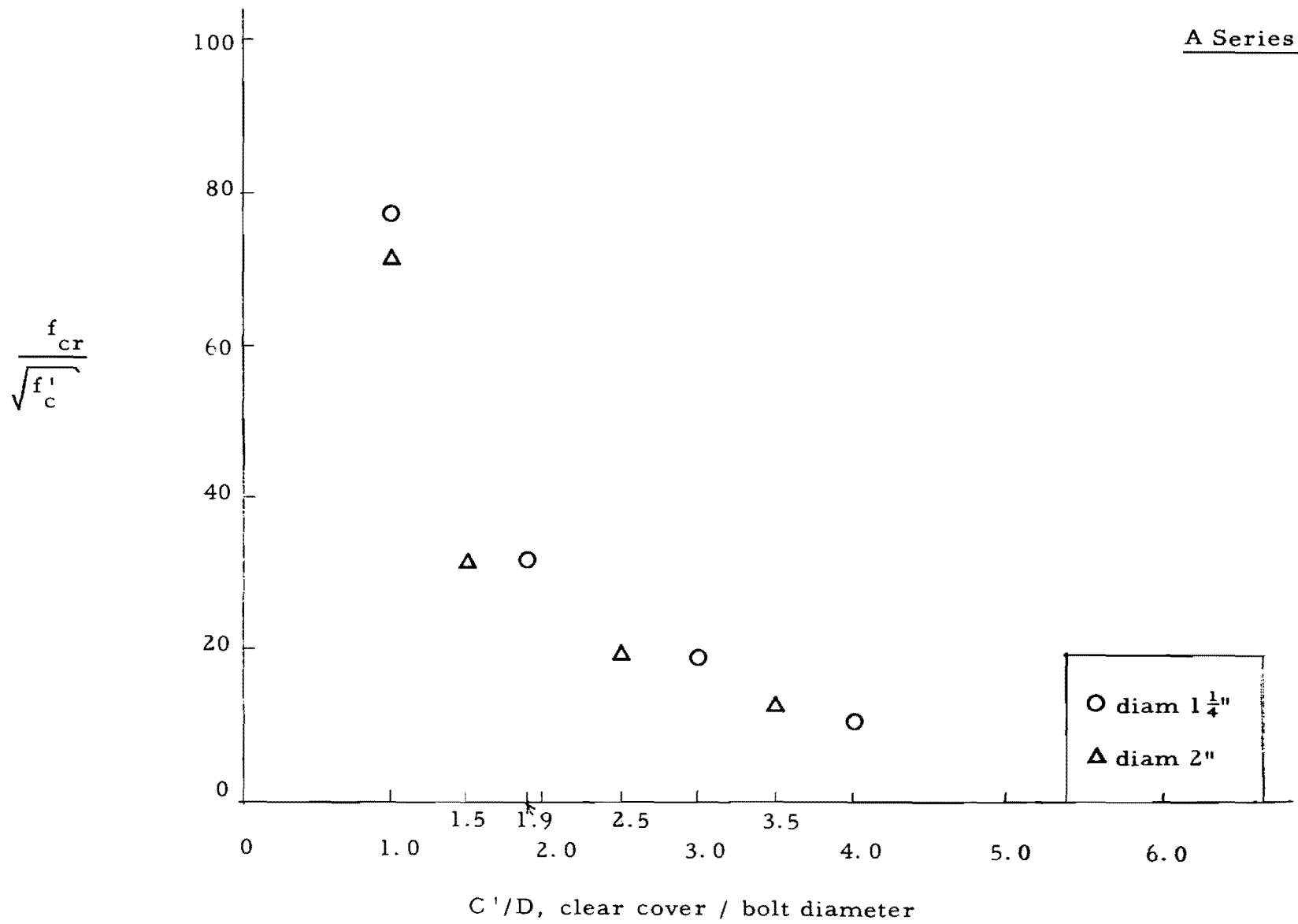


Fig. 25. Critical bearing stress vs ratio of clear cover to bolt diameter (A Series)

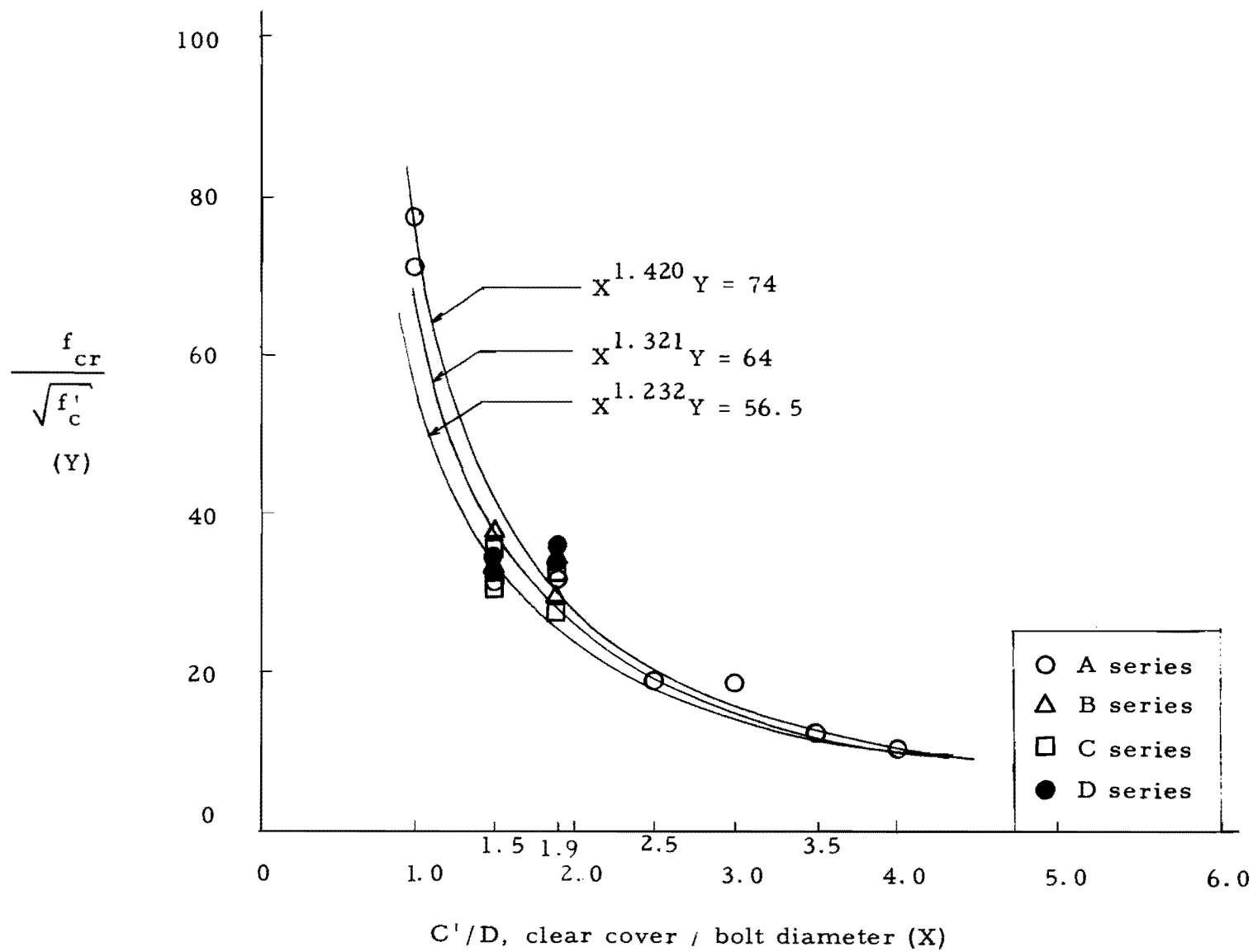


Fig. 26. Critical bearing stress-ratio of clear cover to bolt diameter (A, B, C, D Series)

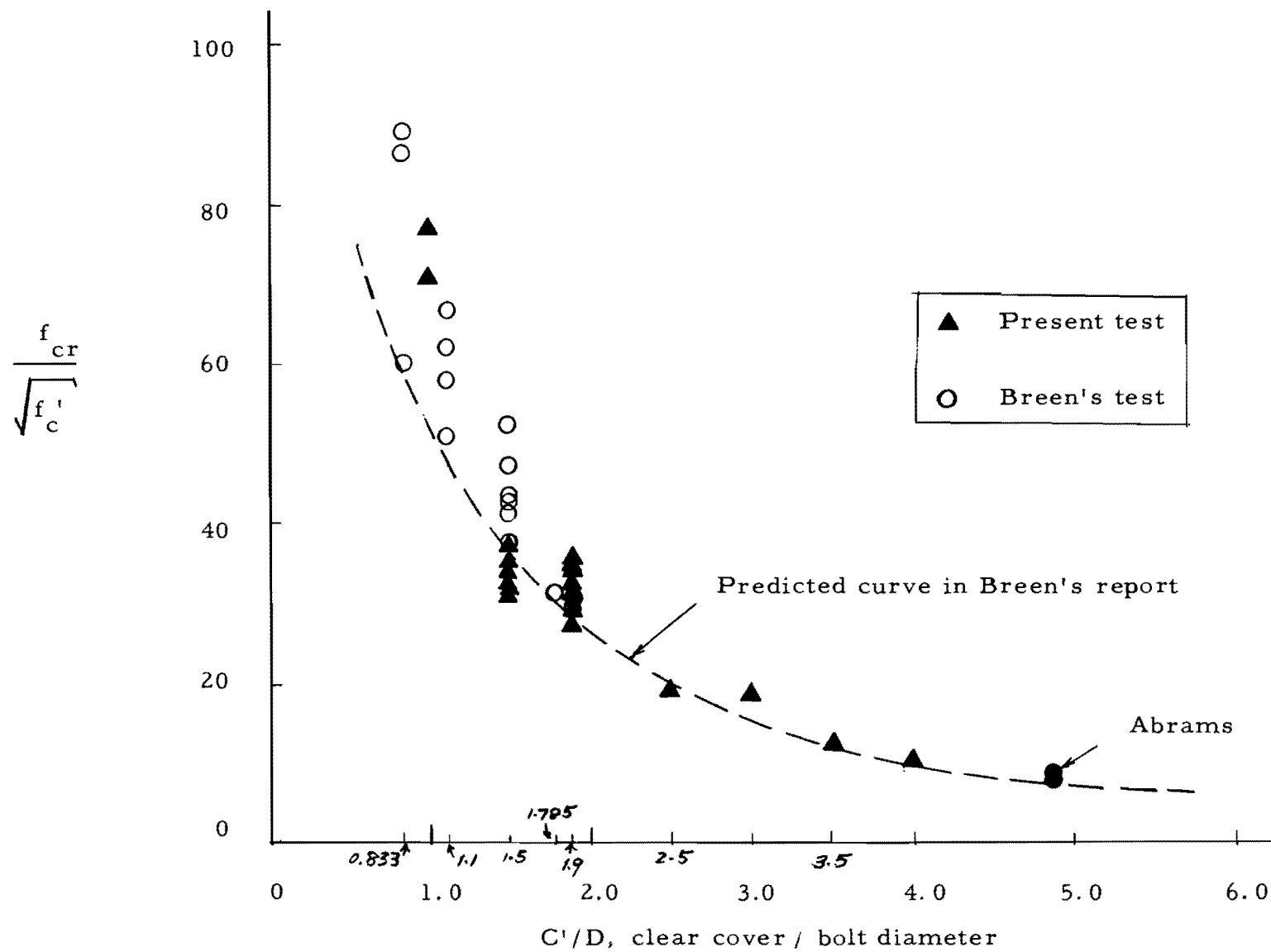


Fig. 27. Critical bearing stress vs ratio of clear cover to bolt diameter
(Present and Breen's tests)

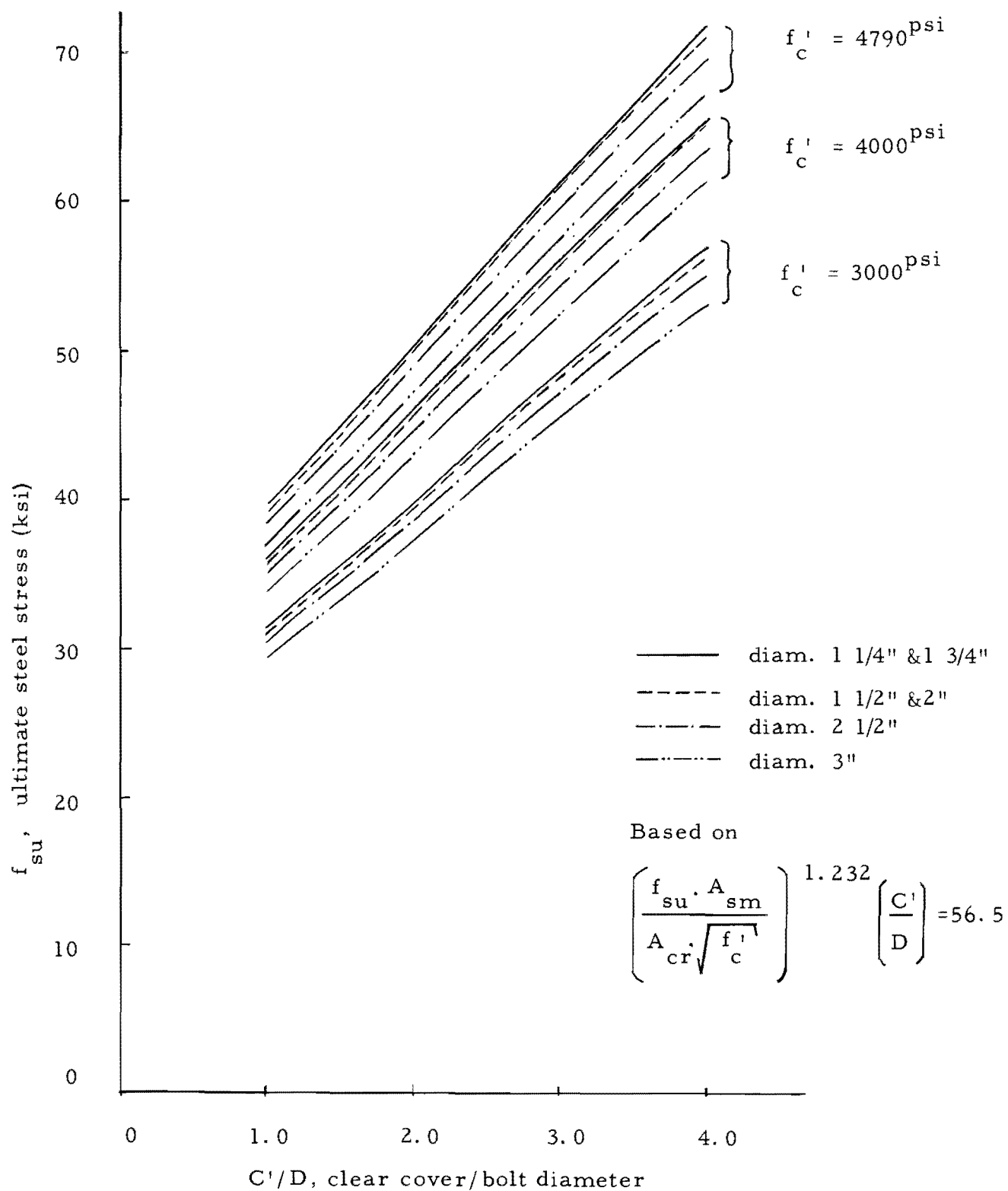


Fig. 28. Ultimate steel stress-ratio of clear cover to bolt diameter relationship

The steel stress versus slip curves for all specimens of the A series are shown in Figs. 29a and b. Considering the wide range of covers represented and the amount of scatter in the data, no conclusive statement can be made about the effect of clear cover ratios on slip at service load levels. It should be noted, however, that at service load levels the values of slip developed were roughly in proportion to the diameter of the bolts. Since the allowable slip in a structural application should be somewhat proportional to the size of the member, this may be an acceptable trend.

Effective Low-cycle Repeated Loading

Fifty cycles of repeated loading were applied to four bolts in this program. An upper steel stress level of 34 ksi was chosen as a moderate overload level for high strength steels, using a safety factor of slightly less than 2. Considering that complete unloading to zero stress was undesirable, a lower stress level of 2 ksi was adopted.

During the repeated loading cycles no cracks were observed on the side faces of the specimen except for the usual flexure cracks which appeared away from the bolt anchorage. However, small cracks did appear on the concrete face around the anchor bolts. As shown in the steel stress versus slip curves of Figs. 30a and 30b, substantial parts of the gross slips were recovered during the repeated loading. The average amount of accumulated slip in 50 cycles was 13 percent of the total slip at the end of the first cycle, with a maximum value of 17 percent. The maximum accumulations of slips were 0.005 inches and 0.0095 inches for the 1½" and 2" anchor bolt specimens, respectively. These values are almost negligible for practical design purposes.

The ultimate strengths for the repeated load series were observed to be a little higher than those for the companion specimens. This was possibly due to the higher concrete strength because of the greater age of the specimens at the time of failure. Since substantial testing time was required for the first specimen of this series (due to the change in testing technique) subsequent tests were unavoidably delayed.

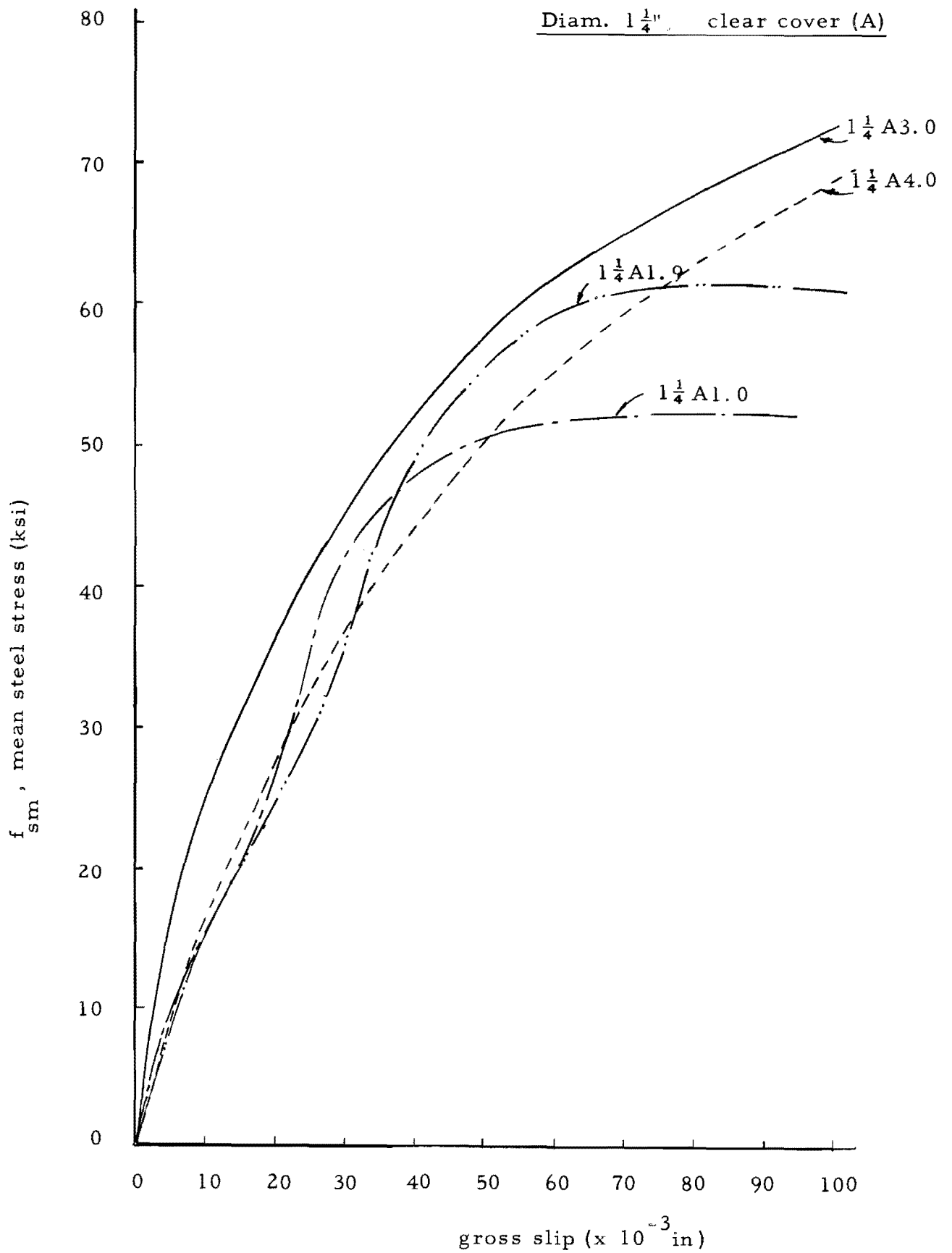


Fig. 29a. Steel stress vs slips curves for A series (diam. $1\frac{1}{4}$ ")

Diam. 2", clear cover (A)

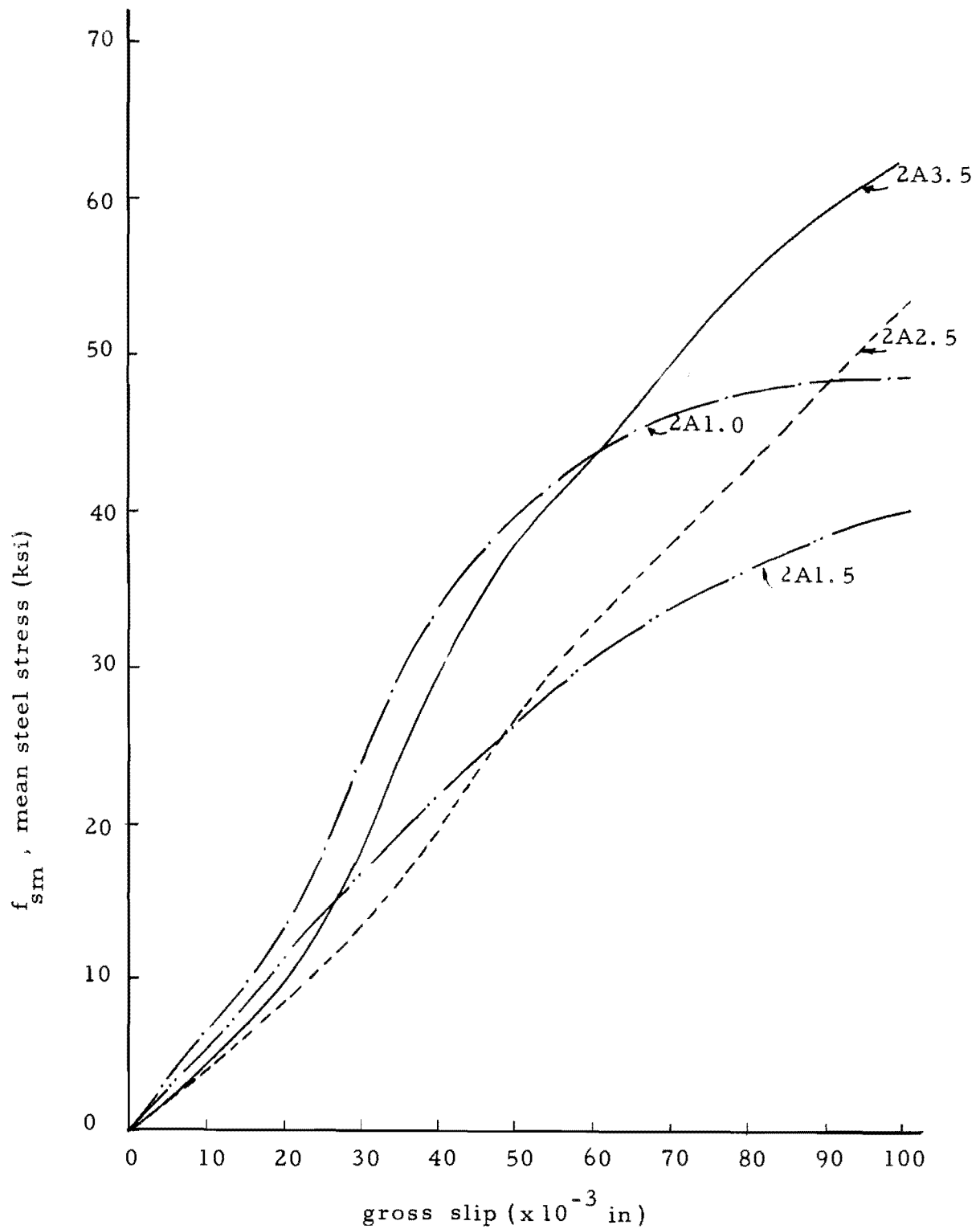


Fig. 29b. Steel stress vs slip curves for A series (diam. 2")

Diam. $1\frac{1}{4}$ ", repeated loading (B)

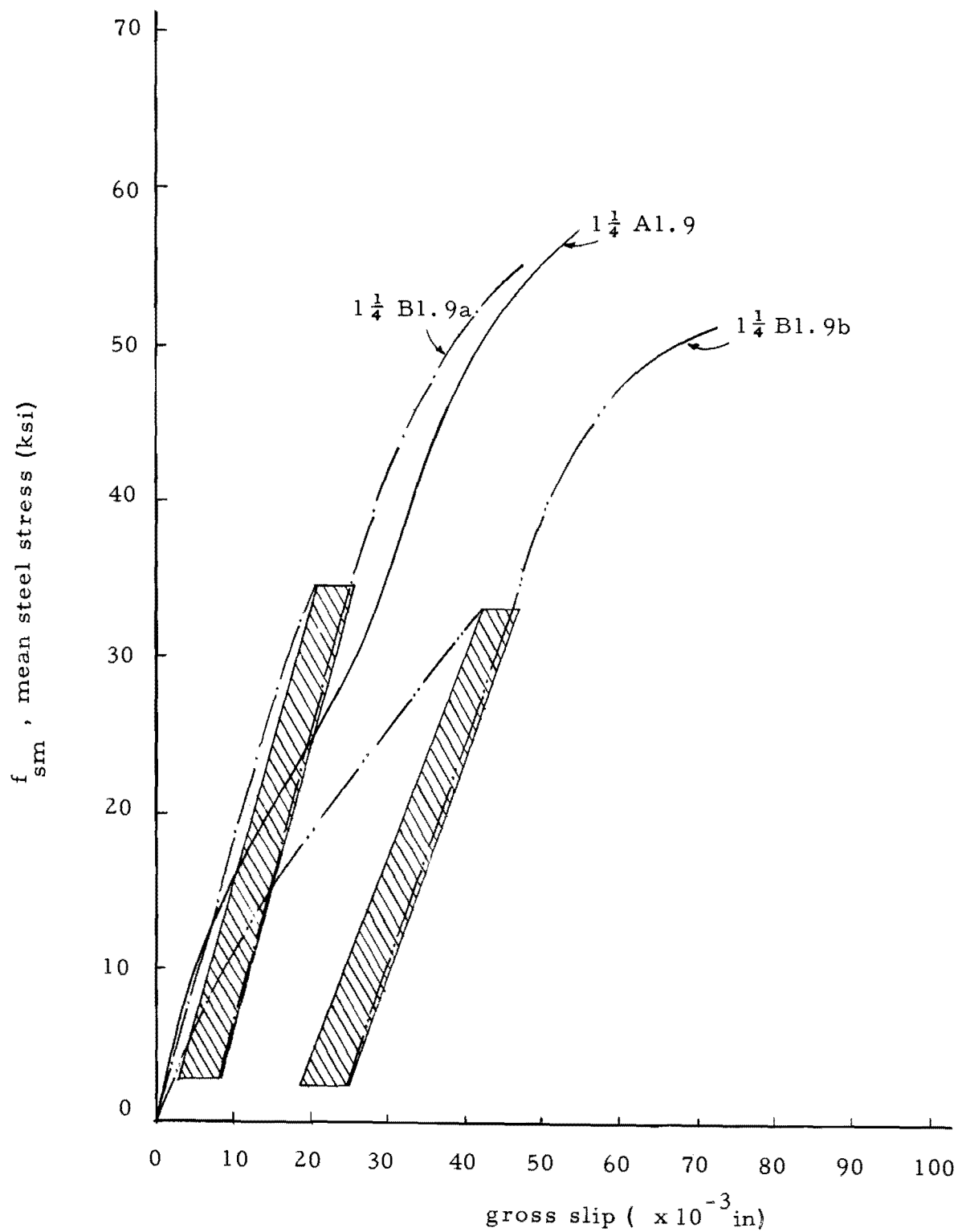


Fig. 30a. Steel stress vs slip curves for B series (diam. $1\frac{1}{4}$ ")

Diam. 2" , repeated loading (B)

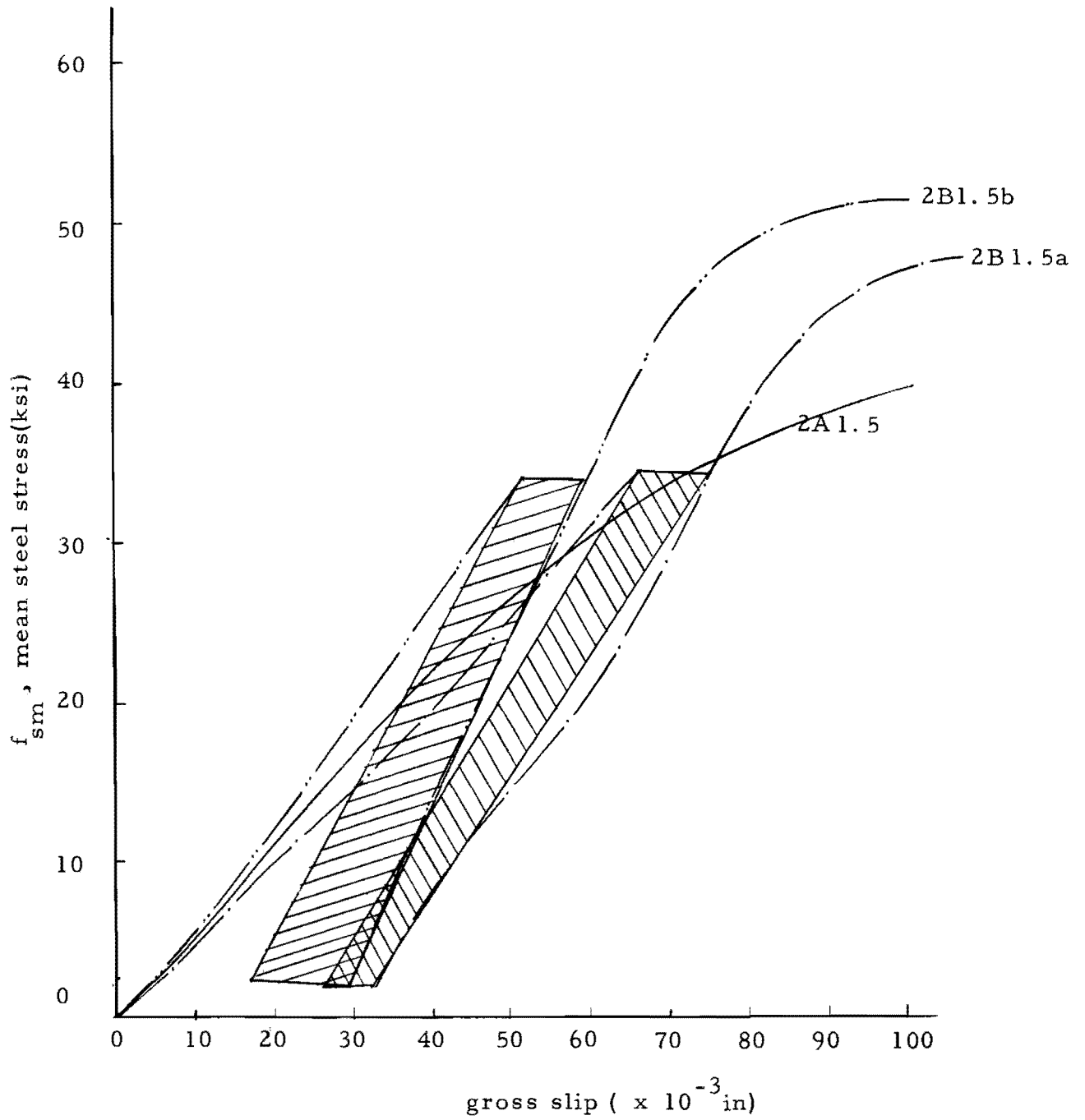


Fig. 30b. Steel stress vs slip curves for B series (diam. 2'')

The results of this limited series provide a significant design check for anchor bolts which are subjected to this kind of loading. It would be highly desirable to investigate the fatigue strength of this type of connection in subsequent research.

Effective Circular Shape

The ultimate strength and behavior of circular specimens were similar to those of the companion rectangular specimens with the exception of the minor difference in the final failure pattern. As shown in Figs. 31a and 31b, the basic pattern was a splitting failure; however, the splitting cracks along the bolt axis were not as definite as in the other series of tests, except for 2C1.5a. The general failure pattern was classified as edge splitting as previously explained. The average ultimate steel stresses of the 1½" and 2" anchor bolts were 63.9 ksi and 42.3 ksi, respectively, whereas those of the companion rectangular specimens were 60.1 ksi and 43.0 ksi. Thus this series of tests indicates that there was no reduction of ultimate strength due to the circular shape of the specimens.

Steel stress versus slip curves are shown in Figs. 32a and 32b. Comparison with the values obtained from the rectangular specimens of series A indicates no definite adverse effect due to shape for two of the specimens, although some adverse effect was found for the other two bolts.

Comparison of the computed ultimate bearing stresses with those obtained in the comparable rectangular specimen indicates no adverse effect due to shape. The semi-rational assumption used in deriving the fictitious bearing stress relationship would indicate the same value for a square or a circular shaft and these values seem to confirm the hypothesis. This test series indicates that there is no significant effect of circular shape on the ultimate strength and behavior as compared to equivalent rectangular shafts.

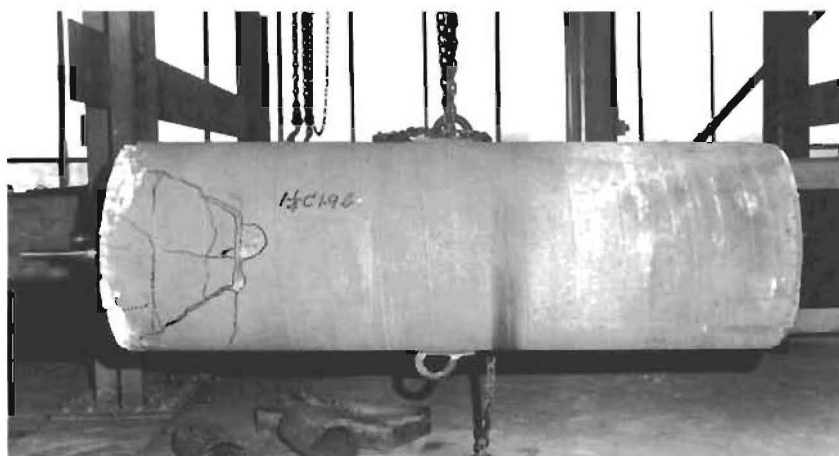


Fig. 31a. Failure of C series (1 1/4" diam. bolts)

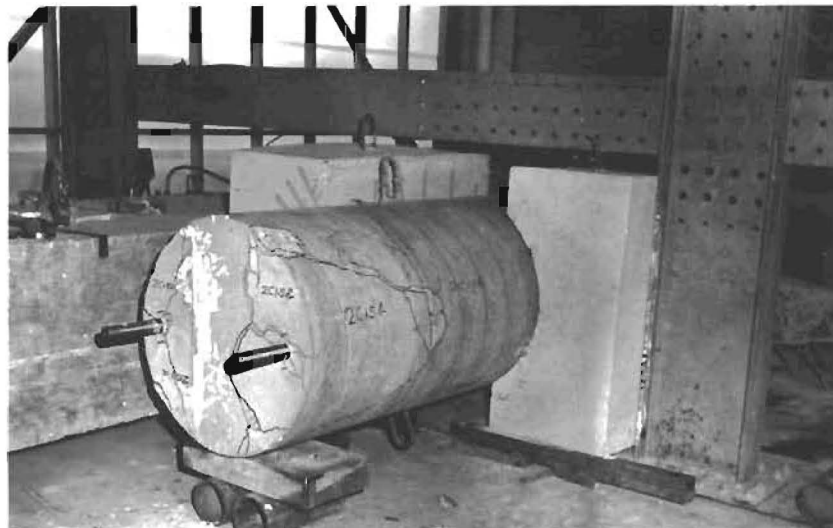
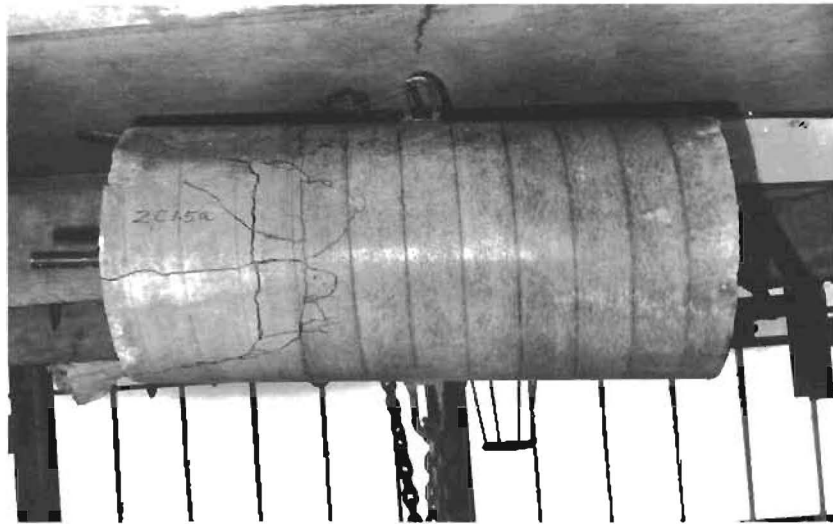


Fig. 31b. Failure of C series (2" diam. bolts)

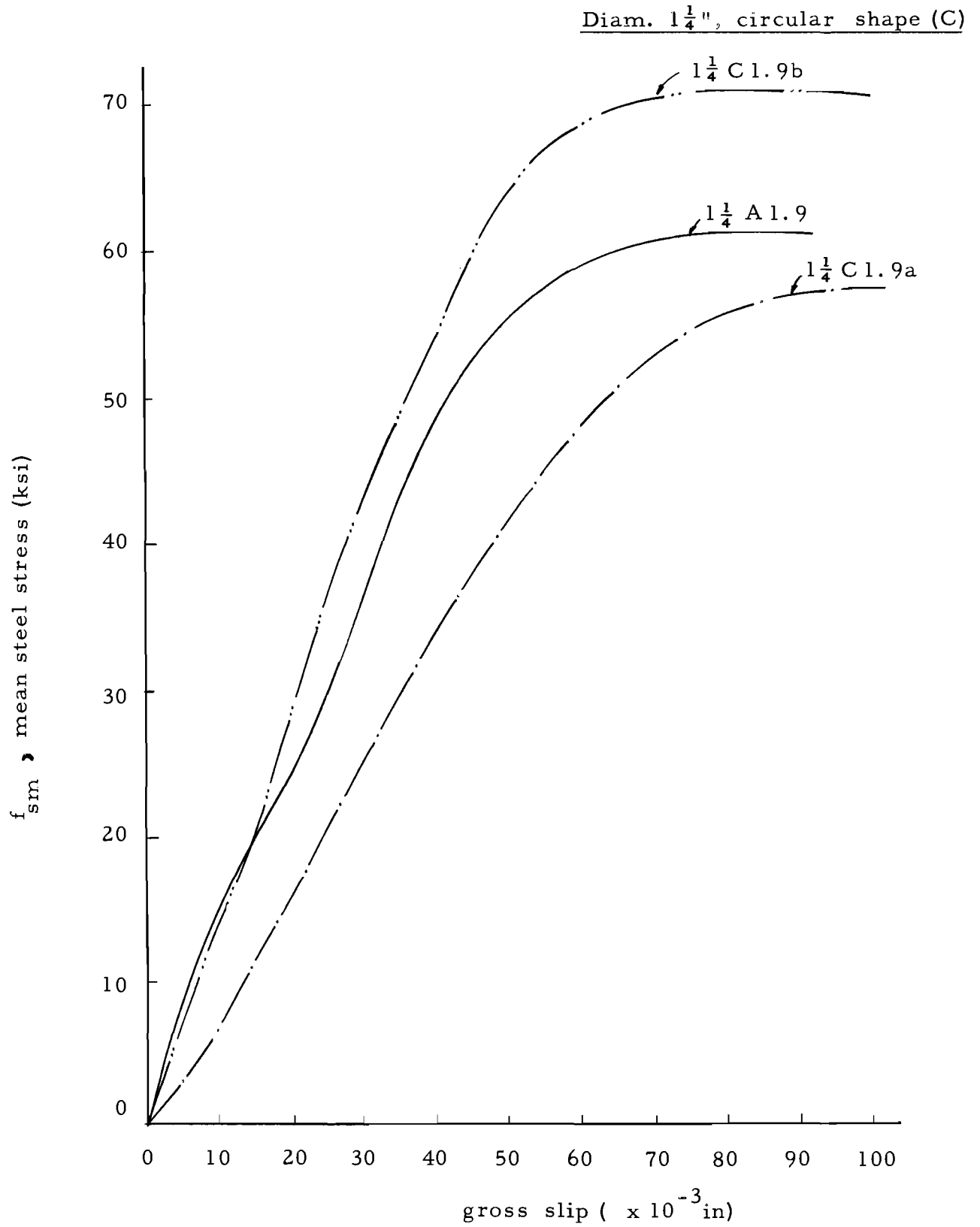


Fig. 32a. Steel stress vs slip curves for C series (diam. $1\frac{1}{4}$ ")

Diam. 2", circular shape (C)

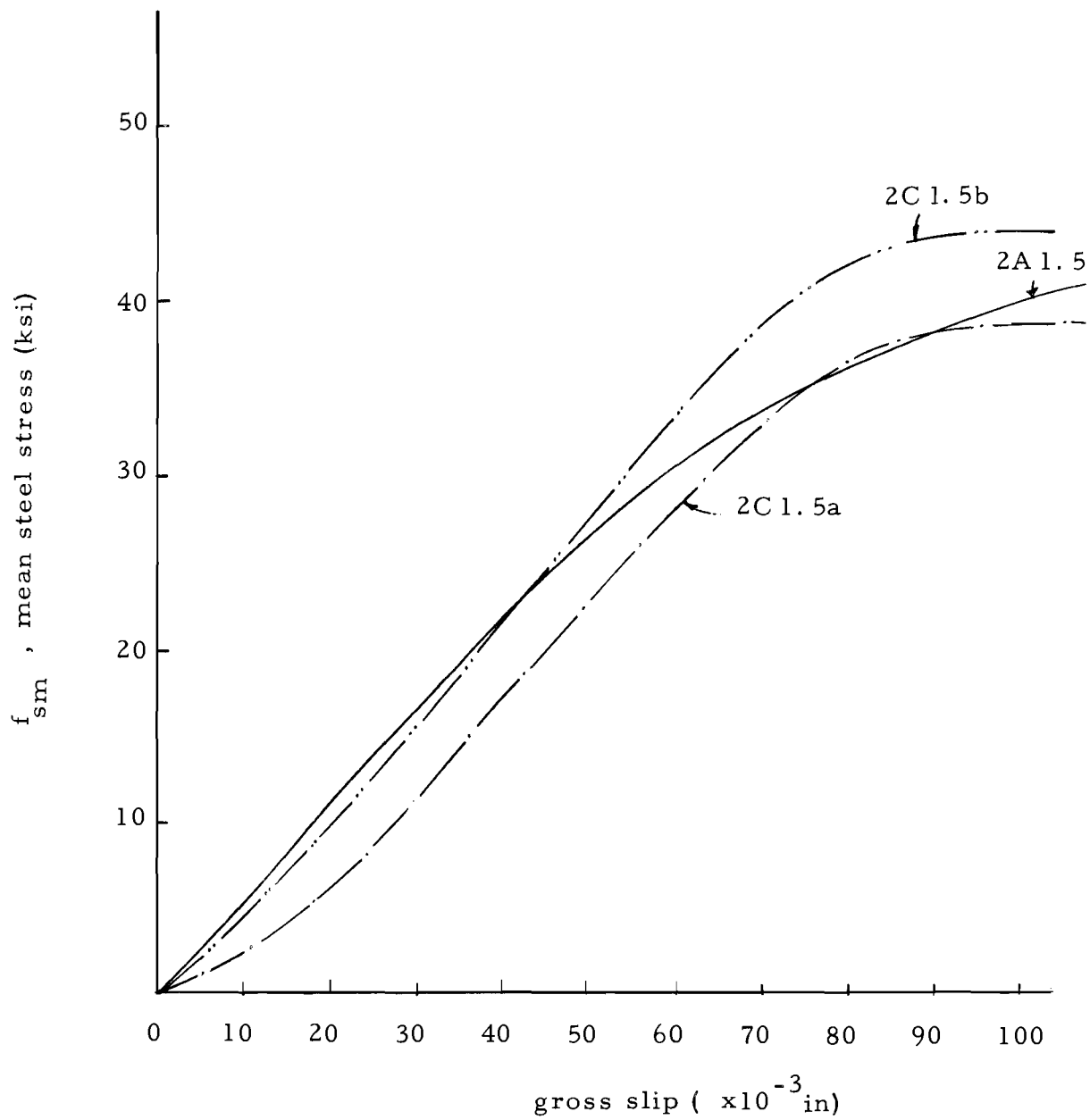


Fig. 32b. Steel stress vs slip curves for C series (diam. 2")

Effect of Low-concrete Strength

For this series of tests the compressive strength of the concrete was purposely chosen to be approximately 2500 psi, although the actual strength obtained was slightly lower than this design strength. The developed ultimate steel stresses of the specimens of this series and the corresponding specimens of series A are given in Table 1. The average strength reductions are 20 and 31 percent for the 1½" and 2" anchor bolt specimens, respectively. The reductions were much less than the tabulated decrease in concrete strength and are close to the 27 and 35 percent reductions predicted by assuming f_{cr} varies as $\sqrt{f'_c}$.

TABLE 1 CONCRETE STRENGTHS AND ULTIMATE
STEEL STRESSES OF D SERIES

Specimen	f'_c			f_{su}	
	psi	%	$\sqrt{\% \times 100}$	ksi	%
1½ A1.9 (Companion)	4610	100	100	60.1	100
1½ D1.9a	2460	53	73	49.9	83
1½ D1.9b	2460	53	73	47.3	78
2 A1.5 (Companion)	5240	100	100	43.0	100
2 D1.5a	2240	42	65	28.8	67
2 D1.5b	2240	42	65	30.4	71

The observed yield stress versus slip relationships for these specimens are shown in Figs. 33a and 33b. The slips measured below the steel stress of 20 ksi are approximately the same as those of companion specimens of series A. Above the steel stress level of 20 ksi the slips start to deviate rapidly in comparison with the higher strength concrete specimens.

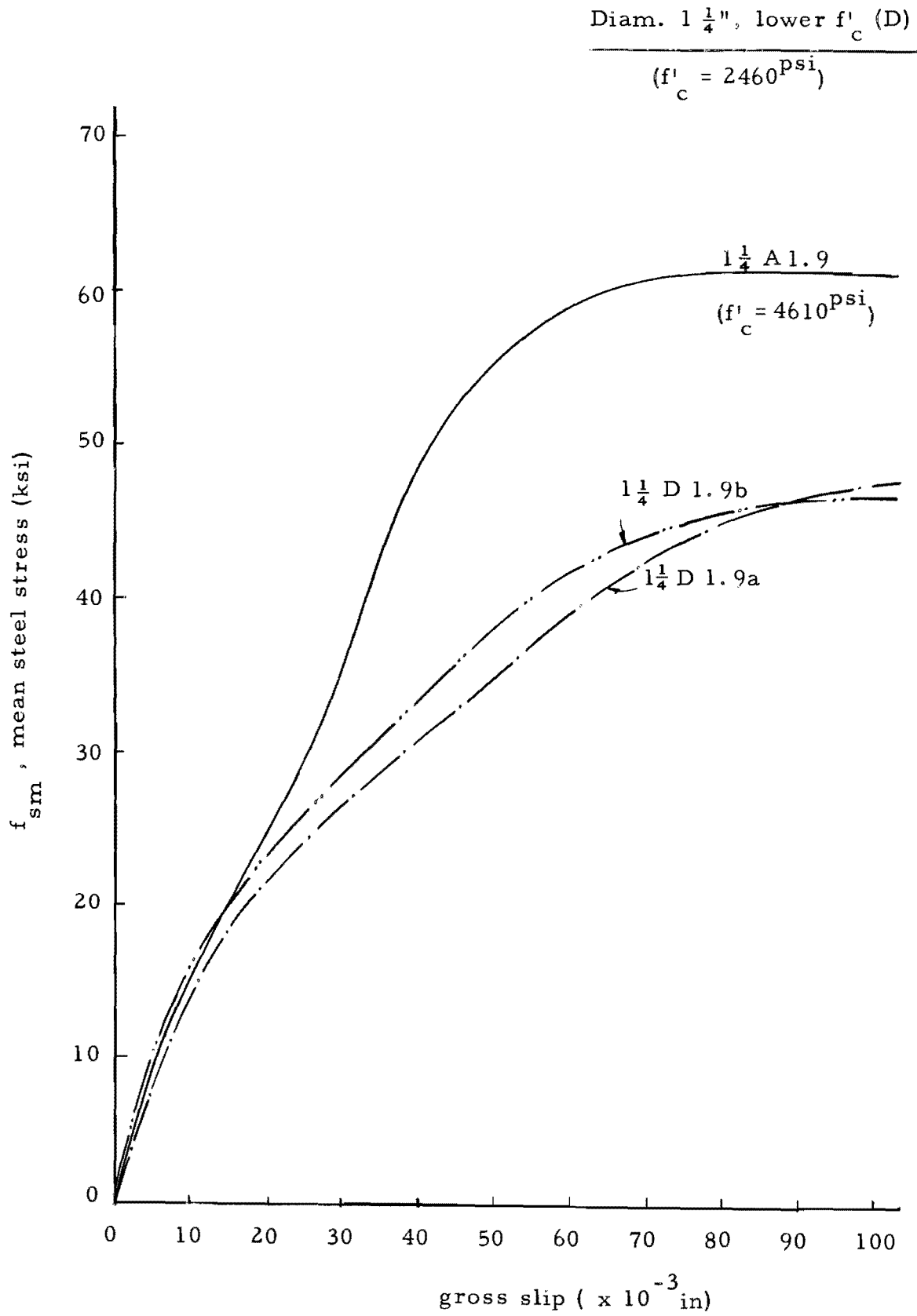


Fig. 33a. Steel stress vs slip curves for D series (diam $1 \frac{1}{4}$ ")

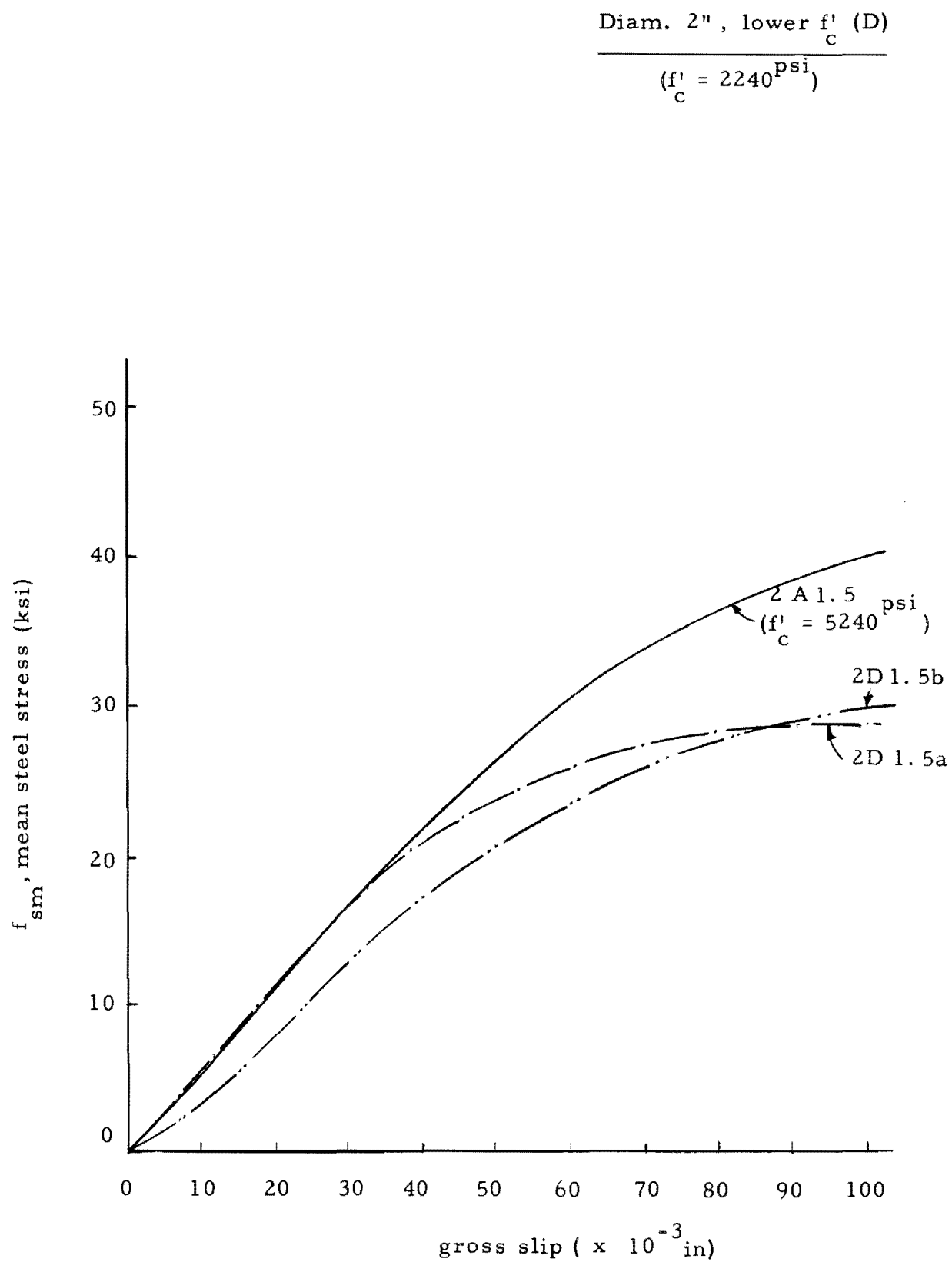


Fig. 33b. Steel stress vs slip curves for D series (diam. 2")

It is probable that internal concrete cracking begins to develop extensively in the low concrete strength specimens at about this stress level. As shown in Fig. 9, some shrinkage cracks in the vicinity of the bolt opened up prior to testing the 2" anchor bolt specimen; however, test results showed no adverse effects of shrinkage cracks on the ultimate strength and slip response.

This series demonstrates low concrete strength will cause low ultimate bolt strength approximately in proportion to the square root of the concrete strengths. In addition, the steel stress-slip response curves are adversely affected above normal service load levels.

Effect of 90-Degree Bends

In a very limited test series, two bolts of each size were tested with 90-degree bends and bolt extensions in place of nut anchorages. The details of the bends are shown in Fig. 5 and the arrangement of the bolts in the specimen is shown in Figs. 3 and 4. The bent portions of the bolts were placed along a radius towards the center of the shaft.

For this test series two different failure patterns were observed. As shown in Fig. 16, the 1½" anchor bolts with 2-3/8" clear cover failed with primary crushing of the concrete cover over the bolt anchorage and with cracks developing in radial directions above the bolt anchorage. No splitting cracks directly above the bolt axis appeared. In contrast, the 2" anchor bolts, with 3" of clear cover had a typical splitting failure, as shown in Fig. 34. It is possible that the basic geometric characteristics placing the major portion of the bearing area farther from the surface in the 2" specimen caused this very significant change in failure patterns.

As shown in Fig. 24, the average ultimate steel stresses were 50.1 ksi for the 1½" bolts and 47.3 ksi for the 2" bolts. This means a strength reduction of approximately 17 percent for the smaller size bolts and a strength increase of 10 percent for the larger size bolts, with respect to the companion specimens of series A. These variations may be somewhat influenced by variations in the concrete strengths of the two specimens, but examination of

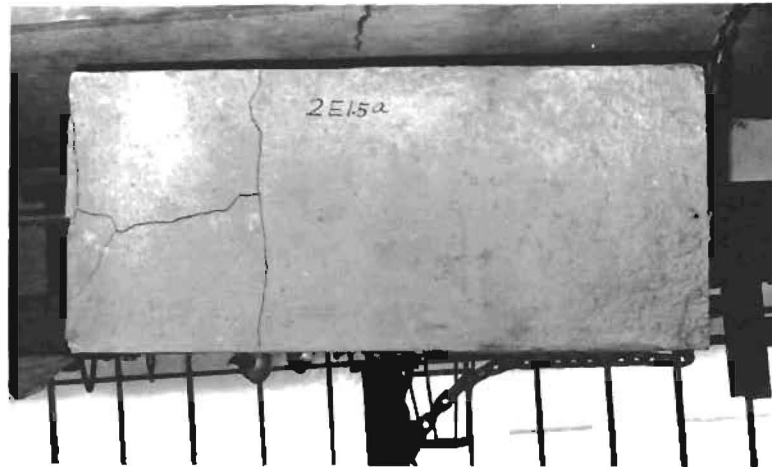


Fig. 34. Failure of E series (2" diam. bolts)

the concrete strengths indicate that we would expect the opposite effect. Until a suitable failure hypothesis for a bent bolt can be developed, this apparent contradiction cannot be explained.

Figures 35a and 35b compare the slip curves for the bent bolts with the companion specimens having nut anchorages. The two curves of steel stress versus slip for the $1\frac{1}{4}$ " anchor bolts are almost identical and both deviate substantially from the results with nut anchors even at very low steel stress levels. At a nominal steel stress of 20 ksi the observed slip for the bent bolts was almost twice as large as that of the companion specimen. In contrast, the slip measurements for the 2" bolt seem inconclusive because one of the curves is almost identical to the companion specimen, while the other deviates greatly for stress values above 15 ksi. The only difference observed during the tests between these two specimens was that somewhat more cracks were observed in 2A1.5b, as shown in Fig. 34. This tends to confirm the presence of larger slips in specimens undergoing crushing type failures.

The present test used only limited bend details and is too restricted in scope to be conclusive. It would be desirable to further study the effect of bend details on ultimate strength and behavior of hooked anchor bolts. The somewhat inconclusive evidence of this series indicates that the hooked bolt is not very effective in resisting slip at service load levels when compared to bolts with simple nut anchorages.

Conclusions

The investigation presented was a limited study of six factors affecting the development of high strength anchor bolts. The test series included high strength anchor bolts of $1\frac{1}{4}$ " and 2" diameter with embedment lengths of 10 diameters. Except for the bent bolts the bolts were anchored with a standard nut. Only a limited range of variables was investigated; hence all conclusions must be restricted to this range of physical dimensions.

Diam. $1\frac{1}{4}$ " , 90° bend (E)

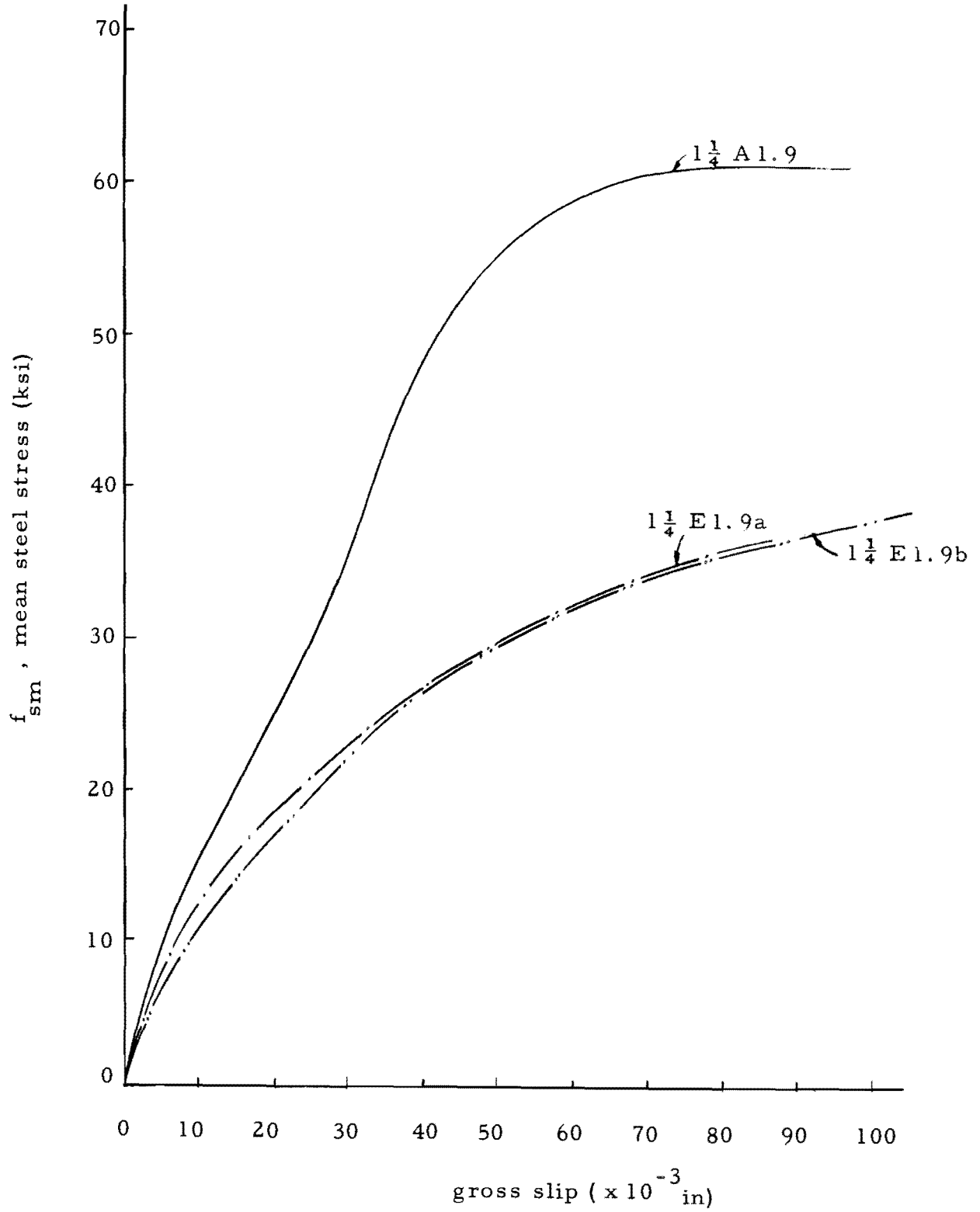


Fig. 35a. Steel stress vs slip curves for E series (diam. $1\frac{1}{4}$ ")

Diam. 2", 90° bend (E)

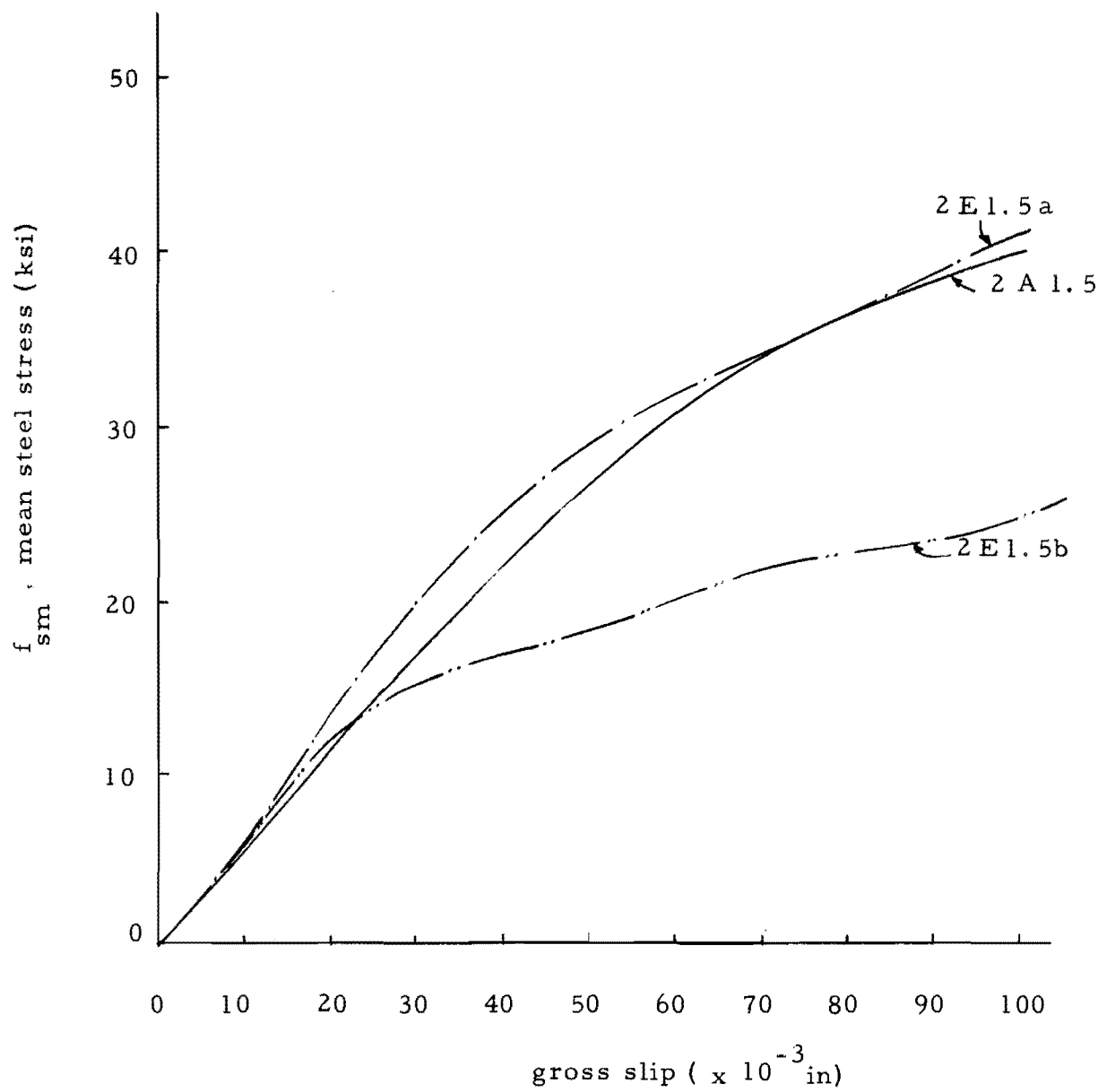


Fig. 35b. Steel stress vs slip curves for E series (diam. 2 ")

From this investigation the following conclusions may be drawn:

1. The method of loading the shaft specimen had a very significant effect on the behavior of the anchor bolt. The loaded end slip was almost tripled when no lateral load was applied in the length of the bolt, but the ultimate strength was essentially of the same magnitude.
2. The amount of concrete cover over the anchor bolt was an important factor in the development of the tensile strength of the bolt. However, it did not show any significant effect on the slip behavior. For a given concrete strength and a given size of bolt, the required amount of cover was correlated with the developable tensile strength of the bolt, using the expression

$$(f_{cr} / \sqrt{f'_c})^{1.232} (C'/D) = 56.5$$

3. Application of the design expression given above would indicate that very large clear cover to bolt diameter ratios are necessary to develop 60 ksi yield point anchor bolts. The series A test results indicate that clear covers almost double the bolt diameter were usually insufficient to develop the nominal yield.
4. The concrete strength was a decisive factor affecting ultimate strength and behavior. Low concrete strengths caused a definite reduction of developable ultimate strength and resulted in poorer slip response.
5. The circular shape of drilled shafts did not significantly affect the ultimate strength or slip behavior when compared with rectangular shape.
6. The low-cycle repeated loading of the type adopted in this investigation showed very limited harmful effects.

7. The limited series of tests with 90-degree bends showed that the particular length of hook used in this program was not as effective as a standard nut anchor in developing positive slip resistance.

APPENDIX

TABLE A SUMMARY OF DATA

Specimen	f'_c psi	Age of test days*	Slip $\times 10^{-3}$ in.			f_{su} ksi	Failure ^a pattern	f_{cr} psi	$\frac{f_{cr}}{\sqrt{f'_c}}$	jd in.
			$f_{sm}=20$ ksi	$f_{sm}=34$ ksi	$f_{sm}=60$ ksi					
1½A1.0	4580	7	13	24.2		52.9	C	5220	77.1	16-1/2
1½A1.9	4610	7	14.5	28.5	61	60.1	C+S	2160	31.8	17-3/4
1½A3.0	4610	7	7	17.7	54.5	76.5	S	1259	18.5	17-7/8
1½A4.0	4580	7	14.4	27.5	71.4	70.7	S	698	10.3	17
1½B1.9a	5270	12		19.5-23.5**		59.3	C+S	2130	29.3	17-3/4
1½B1.9b	5480	13		42 - 47**		71.9	C+S	2580	34.8	11-3/4
1½C1.9a	5630	7	24	40		57.3	E	2050	27.4	18
1½C1.9b	5990	8	15	23.3	46.2	70.5	E	2530	32.7	10-3/4
1½D1.9a	2460	7	17	47.5		49.9	S	1790	36.0	17-3/4
1½D1.9b	2460	7	15	41		47.3	S	1698	34.2	17-15/16
1½E1.9a	5160	14	25.5	70		50.7	C			17-1/2
1½E1.9b	5160	14	23	68		49.5	C			18-5/16

*Age of specimen (days) on the test date

**Slips of 1st cycle and 50th cycle.

^aC = Crushing; S = Splitting; E = Edge splitting

TABLE A SUMMARY OF DATA (Continued)

Specimen	f'_c psi	Age of test days*	Slip $\times 10^{-3}$ in.			f_{su} ksi	Failure ^a pattern	f_{cr} psi	$\frac{f_{cr}}{\sqrt{f'_c}}$	jd in.
			$f_{sm}=20$ ksi	$f_{sm}=34$ ksi	$f_{sm}=60$ ksi					
2A1.0	4780	7*	26.4	40.5		49.7	C	4940	71.1	21-3/8
2A1.5	5240	8	36	70		43.0	C+S	2280	31.5	22-1/4
2A2.5	5240	8	40	62	116	62.1	C+S	1410	19.4	12
2A3.5	4780	7	31	44.6	92	70.0	S	882	12.7	20-3/4
2B1.5a	5700	14		66-75.5**		47.75	C+S	2530	33.5	21-5/8
2B1.5b	5960	15		51-59**		53.4	C+S	2830	37.5	13-1/2
2C1.5a	4570	7	45	73		39.5	E	2095	31.0	21-1/2
2C1.5b	4640	8	37.7	61		45.2	E	2400	35.2	21
2D1.5a	2240	7	37			28.8	S	1790	32.3	22-1/16
2D1.5b	2240	7	47.6			30.4	S	1698	34.1	22-1/16
2E1.5a	4710	7	30	69.5		48.9	S			21-1/2
2E1.5b	4710	7	60			45.7	S			21-1/4
2F1.5a	5170	7	14	26		54.5	C+S	2890	40.2	21-1/4
2F1.5b	5420	8	14	27	65	60.7	C+S	3220	43.7	21-5/8

*Age of specimen (days) on the test date

**Slips of 1st cycle and 50th cycle

^aC = Crushing; S = Splitting; E = Edge splitting

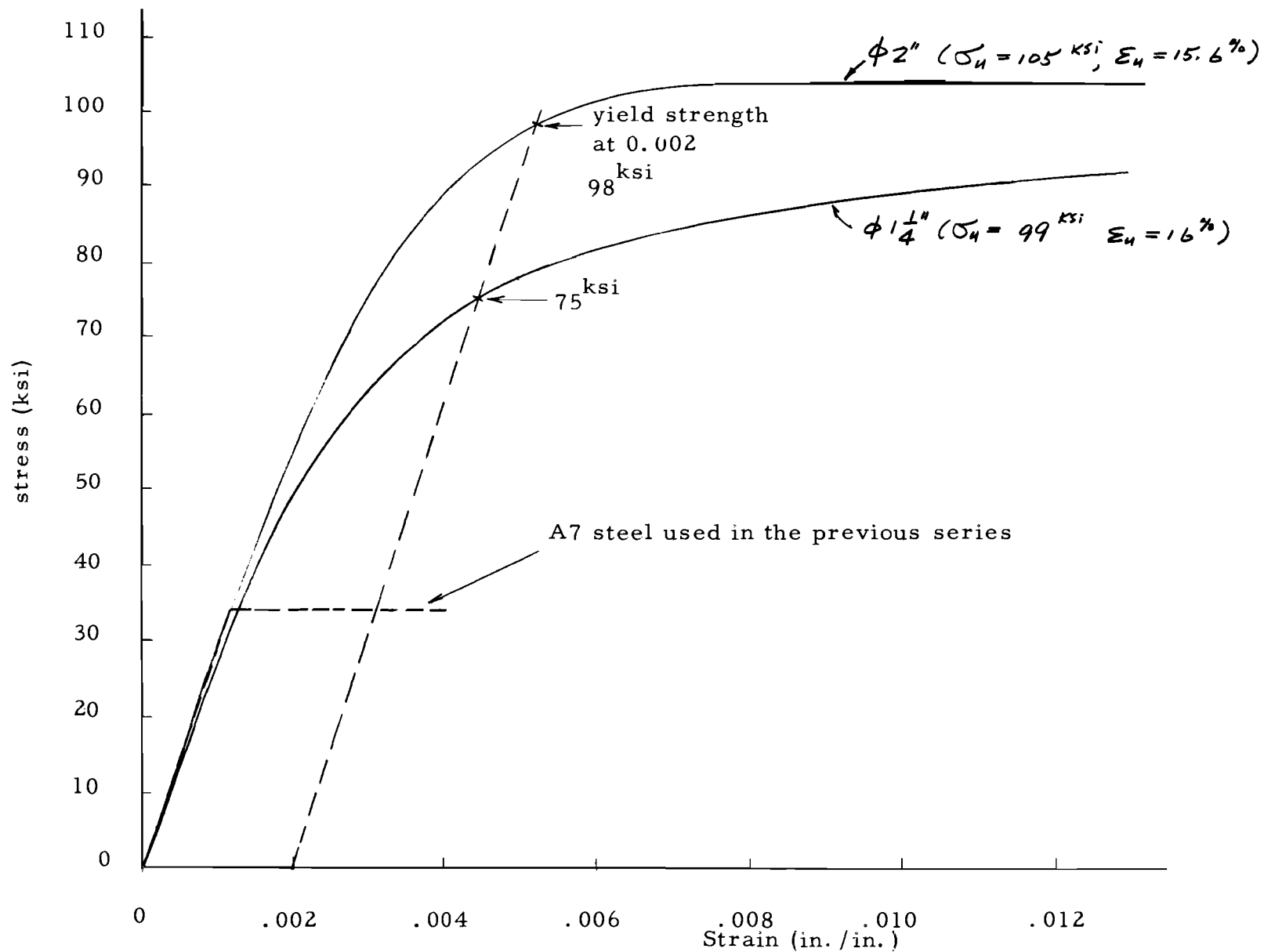


Fig A. High strength anchor bolt stress strain curves (coupon tests)

BIBLIOGRAPHY

1. Abrams, Duff A., "Tests of Bond between Concrete and Steel,"
University of Illinois Engineering Experiment Station
Bulletin No. 71, December, 1913, pp. 97-99.
2. Shoup, Thomas E., and Singleton, Robert C., "Headed Concrete Anchors,"
Proceedings of American Concrete Institute, Vol. 60, 1963,
pp. 1229-1235.
3. Breen, John E., "Development Length for Anchor Bolts," Center for
Highway Research, The University of Texas, April, 1964.
4. Texas Highway Department, Special Provision to Item 421 of "Standard
Specifications for Road and Bridge Construction," January 2, 1962.
5. American Society for Testing Materials, "Standard Specification for
Low-Carbon Steel Externally and Internally Threaded Standard
Fasteners," ASTM A 307-64, 1965 Standards, Part I, p. 222.